THESIS FOR THE DEGREE OF DOCTOR OF PHILOSOPHY

Chemical looping combustion of solid fuels using manganese-based oxygen carriers – investigations in 10 and 100 kW pilots

MATTHIAS SCHMITZ

Department of Space, Earth and Environment

CHALMERS UNIVERSITY OF TECHNOLOGY

Gothenburg, Sweden 2018

Chemical looping combustion of solid fuels using manganese-based oxygen carriers - investigations in 10 and 100 kW pilots

MATTHIAS SCHMITZ

Division of Energy Technology

Department of Space, Earth and Environment

Chalmers University of Technology

Abstract

According to climate simulations, the predicted carbon budget to keep global warming below 1.5°C with high certainty will be used up in 2021, assuming 2017 emissions. As an emissions overshoot seems inevitable, bioenergy with carbon capture and storage (BECCS) has been proposed as a means of removing CO_2 from the atmosphere in the future. This is done by utilizing biomass in combustion processes and storing the resulting CO_2 in underground geological formations such as aquifers or depleted oil- and gas fields, thus rendering the total net emissions of CO_2 negative.

While first generation CCS technologies rely on energy-intensive active gas separation, chemical looping combustion (CLC) can omit that step by utilizing solid metal oxide particles to transfer oxygen from combustion air to fuel, making CO_2 capture inherent to the process and avoiding thermodynamic energy penalties. A key research issue is to find oxygen carriers which perform satisfactorily with respect to fuel conversion and lifetime. Manganese materials are promising candidates from a thermodynamic point of view, potentially cheap and environmentally benign, but have previously been challenged with lifetime issues.

The aim of this work is therefore to find and test manganese-based oxygen carrier materials with good conversion properties and high durability and to identify the process parameters influencing gas conversion and particle lifetime. To do so, the performance of six different oxygen carrier materials was investigated in continuous 10 kW and 100 kW pilots using both fossil and biomass fuels. Performance – with respect to fuel conversion – of all oxygen carriers was higher than that of the state-of-the-art material, i.e. ilmenite. Manufactured materials generally performed better and had a higher lifetime than that of natural materials, an advantage which in utility scale would have to be weighed against their higher cost.

The results suggest that manganese materials, both manufactured and of natural origin, can be a feasible, efficient and cost-effective alternative as oxygen carrier in chemical looping combustion.

Keywords: carbon capture and storage, chemical looping combustion, CLOU, manganese ores, BECCS

List of Publications

This thesis is based on the following publications:

Paper I   Schmitz M, Linderholm C, "Performance of Calcium Manganate as Oxygen Carrier in Chemical Looping Combustion of Biochar in a 10 kW pilot", *Applied Energy* **169**, 2016, 729–737

Paper II   Schmitz M, Linderholm C, Lyngfelt A, "Chemical Looping Combustion of Sulphurous Solid Fuels Using Spray-dried Calcium Manganate Particles as Oxygen Carrier", *Energy Procedia* **63**, 2014, 140–152

Paper III   Schmitz M, Linderholm C, Hallberg P, Sundqvist S, Lyngfelt A, "Chemical-looping combustion of solid fuels using manganese ores as oxygen carriers", *Energy and Fuels* **30**, 2016, 1204–1216

Paper IV   Schmitz M, Linderholm C, Lyngfelt A, "Chemical looping combustion of four different solid fuels using a manganese-silicon-titanium oxygen carrier", 2018, *International Journal of Greenhouse Gas Control* **70**, 2018, 88-96

Paper V   Schmitz M, Linderholm C, "Chemical looping combustion of biomass in 10 and 100 kW pilots - Analysis of conversion and lifetime using a sintered manganese ore", 2018, *submitted for publication*

Contribution report:

Paper I, II and IV: principal author, responsible for the experimental work and data evaluation.

Paper III: principal author, responsible for data evaluation and parts of the experimental work.

Paper V: principal author, responsible for parts of the experimental work and data evaluation.

Related publications not included in this thesis:

- Linderholm C, Schmitz M, Knutsson P, Källén M, Lyngfelt A, "Use of low-volatile solid fuels in a 100 kW chemical-looping combustor", *Energy and Fuels* **28**, 2014, 5942–52.

- Linderholm C, Schmitz M, "Chemical-looping combustion of solid fuels in a 100kW dual circulating fluidized bed system using iron ore as oxygen carrier", *Journal of Environmental Chemical Engineering*, **4**, 2016, 1029–1039

- Linderholm C, Schmitz M, Knutsson P, Lyngfelt A, "Chemical-looping combustion in a 100-kW unit using a mixture of ilmenite and manganese ore as oxygen carrier", *Fuel* **166**, 2016, 533–542

- Linderholm C, Knutsson P, Schmitz M, Markström P, Lyngfelt A, "Material balances of carbon, sulfur, nitrogen and ilmenite in a 100 kW CLC reactor", *International Journal of Greenhouse Gas Control* **27**, 2014, 188–202

- Linderholm C., Schmitz M, Biermann M, Hanning M, Lyngfelt A, "Chemical-looping combustion of solid fuel in a 100 kW unit using sintered manganese ore as oxygen carrier", *International Journal of Greenhouse Gas Control*, **65**, 2017, pp. 170-181

- Linderholm C, Schmitz M, Lyngfelt A, "Estimating the solids circulation rate in a 100-kW chemical looping combustor", *Chemical Engineering Science*, **171**, 2017, pp. 351-359

Acknowledgement

I would like to express my thanks to my supervisor Prof. Anders Lyngfelt, whose enthusiasm and total commitment to both his research and his PhD students have made a great impression on me. My co-supervisor Assistant Prof. Carl Linderholm, thank you for all your help and guidance. Also, thanks for your patience listening to me complaining and for all the good laughs we had.

All my colleagues and friends in the CLC group: Malin, Jesper, Patrick, Ivan, Viktor, Tobias, Magnus, Henrik, Fredrik and Pavleta. Thank you – and all former group members – for good cooperation and interesting conversations. Our lab engineer Ulf has taught me a lot and helped me out on very short notice on countless occasions. I cannot thank you enough. Dima, thank you for sharing the office with me, it has always been a pleasure.

I also would like to thank all non-CLC members of the Energy Technology Division. It is a nice place to work, and mostly so because of you! Marie, Katarina and Mia, thank you for always helping us navigate the jungle of administration. Without you, we would all be doomed.

Martin Roggendorf and Stephan Schwinn at RWE Power provided fuel free of charge, thank you for that. The companies Johnson & Johnson and CRC are gratefully acknowledged for inventing every experimental researcher's best friends: duct tape and 5-56.

The support of my friends, both in Sweden and in Germany, has been invaluable. Special thanks to Dr. Dominique Dechambre and Prof. André Bardow. You might not know it, but in different ways you are in part responsible for my pursuing a PhD.

It is easy to take a caring family for granted; thanks to the whole Schmitz-Happe-Stenholm-Lindal-bunch for always being there. My parents, Annegret and Christoph, thank you for all your love, support and encouragement throughout the years. And for letting me make a mess in the workshop occasionally, a process without which I think I never would have become an engineer in the first place. My sons Johannes and Paul. Yes, you have taken my sleep, but in exchange you have given me purpose, context and so much fun. A good deal, I think.

Linnea, my funny, crazy, smart, loving wife. Thank you for being my best friend and for always backing me up. This work is as much yours as it is mine. Jag älskar dig.

Table of Contents

x

1. Introduction

1.1 Observations on Climate Change

Since the 1950s, the earth's climate has been subject to changes which are unprecedented over time scales ranging from decades to millennia [1]. While the atmosphere and the oceans have grown ever warmer, the anthropogenic emission of greenhouse gases has reached new heights every year, with CO_2 responsible for the bulk of the greenhouse effect, see. Fig. 1.
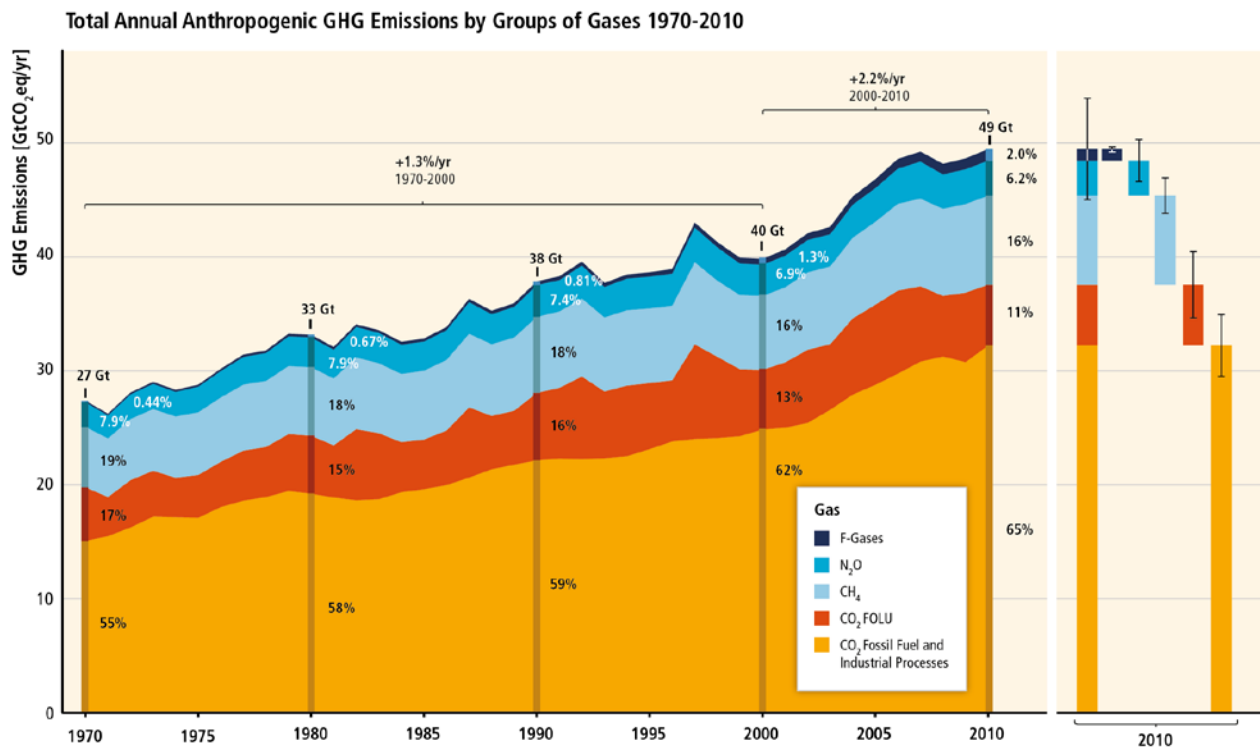
Fig. 1: Total annual greenhouse gas emissions 1970-2010 [2]

The concentration of CO_2 in the atmosphere is to date above 400 ppm, the highest value for at least 800,000 years. Data retrieved from ice core drillings in Antarctica suggest that the CO_2 concentration in the atmosphere correlates well with global temperature changes [3]. On a shorter time scale, atmospheric measurements of CO_2 concentrations and direct temperature measurements support this finding, see Fig. 2.
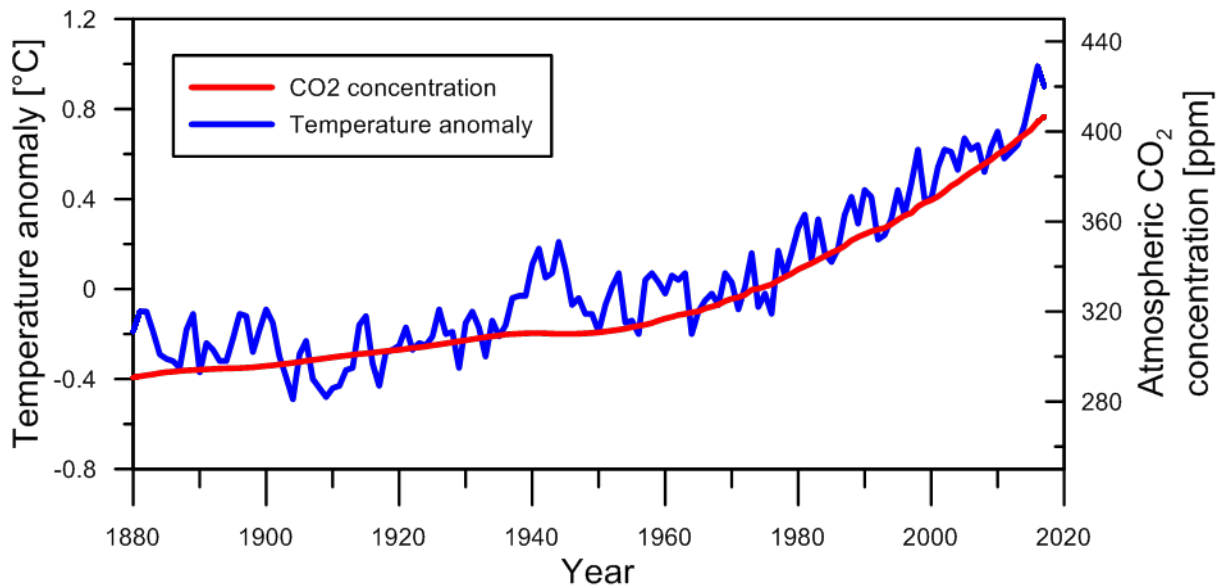
Fig. 2: Annual average CO₂ concentrations and land-based temperature anomalies 1880-2017. Temperature anomalies relative to a 1951-1980 reference period. Data for Temperature anomalies derived from GISTEMP [4], data on CO₂ concentrations from the Law Dome Ice core (1880-1958) [5] and Mauna Loa observatory (1959-2017) [6]

Anthropogenic emissions of CO_2 and other greenhouse gases are thus widely considered to be the major cause of global warming, with 97% of climate scientists agreeing on that paradigm [7]. The greenhouse effect was understood in the middle of the nineteenth century, and the quantitative relation between CO_2 concentration in the atmosphere and earth surface temperature has been known since 1896 [8].

Globally, 2017 was the third warmest year ever recorded – and the warmest without El Niño present – with a surface temperature of 0.84°C above the 20th century average, see Fig. 3. Also, the 17 warmest years since temperature recordings started in 1880 have occurred since 1998, with a new record every third year in the period 1981-2017 [9]. The probability of the observed persisting increase of global temperatures taking place without the presence of anthropogenic influences is lower than 1 in 100,000 [10].
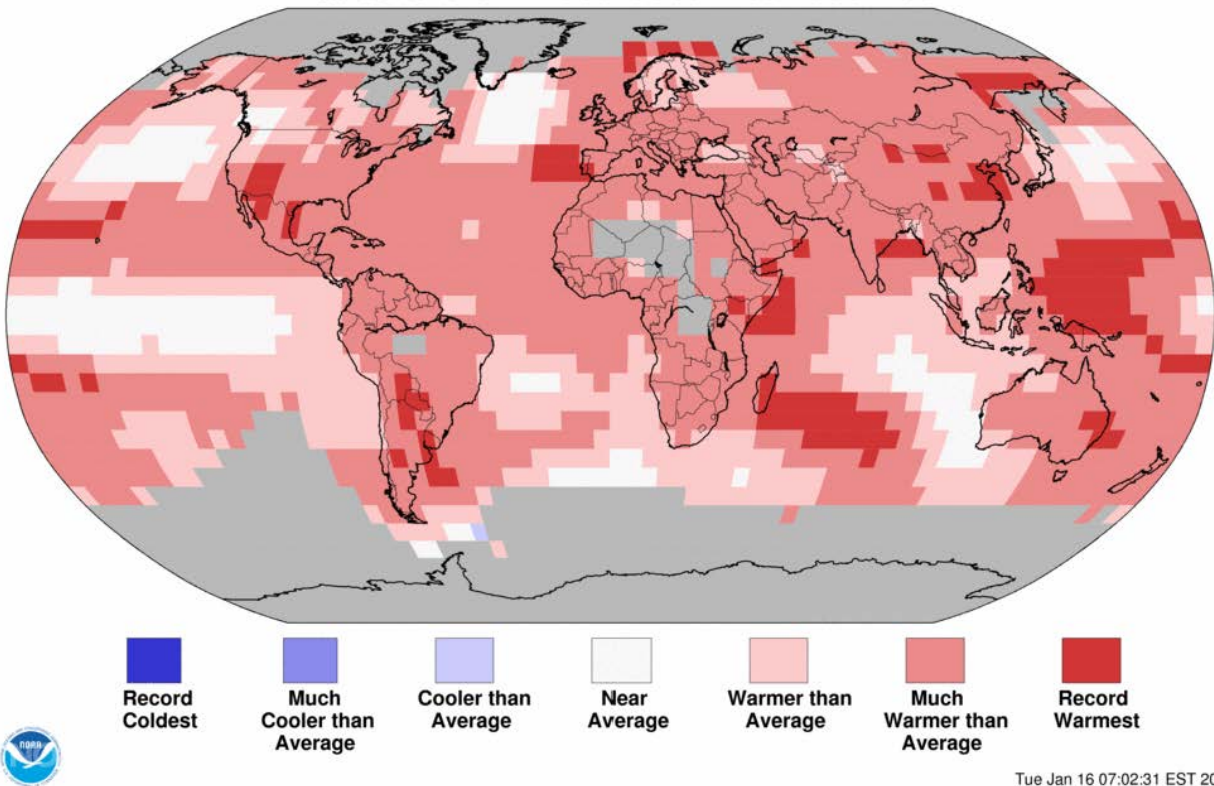
Fig. 3: Global temperature deviations for 2017 [11]

The increase in temperatures has already led to severe consequences: record-high heavy precipitation for the last six decades has been recorded for both dry and wet regions, with a further increase projected for the future [12]. Satellite data indicate that both the Antarctic ice minimum and the Arctic ice maximum in 2017 were the lowest on the 38-year record, i.e. since satellites were first used to investigate earth surface temperatures [13].

In a comparably near future, more severe effects of this kind are likely to occur, considering a predicted increase in surface temperature of 0.9 to 5.4°C, depending on which emission reduction pathways are followed [1]. This would mean an increase which is comparable to the largest naturally occurring climate changes in the last 65 million years in magnitude, but up to a factor 100 more rapid [14].

If no measures for a reduction of greenhouse gas emissions are taken, the consequences for all humankind may be catastrophic. In December 2015, the United Nations Climate Change Conference (COP 21) in Paris thus resulted in 195 countries agreeing to limit the increase in the global average temperature "to well below 2°C above pre-industrial levels and to pursue efforts

to limit the temperature increase to 1.5°C above pre-industrial levels" [15]. The total carbon budget, defined as the amount of CO_2 mankind can emit to reach that goal with 66% probability, is 2250 Gt. To date, over 2100 Gt have already been emitted, leaving an extremely short window of opportunity for reaching the 1.5°C goal: based on global carbon emissions in 2017, this budget will be spent in 2021. The corresponding numbers for the 2°C goal are a total carbon budget of 2900 Gt, which at constant emissions would be spent in 2036 [2].

It should be noted that an increase by 2°C already would mean severe consequences, which is why this threshold is in no way believed to be sufficiently low to preserve status quo, but rather to draw a line between 'dangerous' and 'extremely dangerous' impacts of climate change [16].

1.2 CCS and BECCS

With CO_2 being the most important contributor to greenhouse gas emissions, and most of the emitted CO_2 originating from combustion of fossil fuels for power- and heat production, transportation and industrial purposes [17], one solution to the problem is to eliminate fossil-fuelled combustion processes. Thus, possible ways of decreasing CO_2 emissions are to reduce overall energy consumption or to replace fossil fuels with renewable energy sources. However, these measures are likely insufficient: instead of decreasing, both primary energy use and the use of fossil fuels are expected to go on growing until 2040 according to the International Energy Agency's World Energy Outlook 2017 [18].

A solution which has been proposed to deal with the expected increase of CO_2 emissions is Carbon Capture and Storage (CCS), in which CO_2 is captured from combustion- or industrial processes and permanently stored in deep geological formations. When using CCS with fossil fuels, the process can be made carbon neutral, assuming complete carbon capture. From a CO_2 emissions point of view, the same result can be achieved by conventional biomass combustion: in that case, the generated CO_2 has previously been absorbed from the atmosphere in generating the biomass fuel, i.e. the growth of a plant. If a biomass fuel is used in conjunction with CCS (BECCS, Bioenergy with Carbon Capture and Storage), the net CO_2 balance of the process is negative, see Fig. 4.
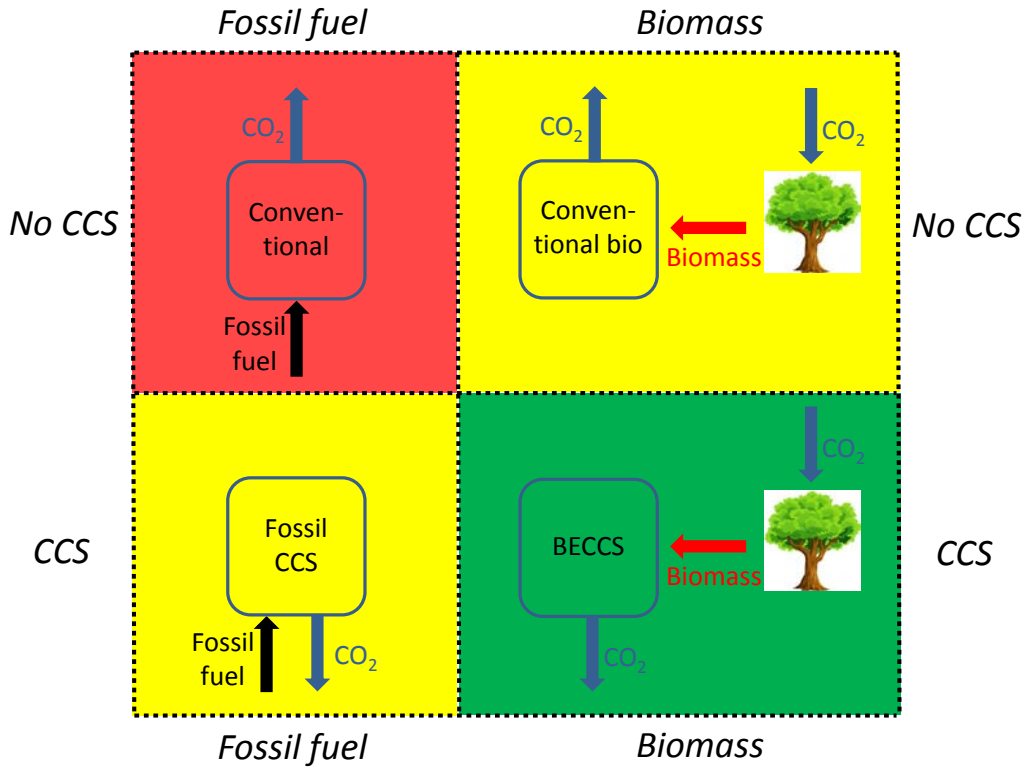
Fig. 4: BECCS compared to other combustion concepts. Green background: net negative CO₂ emissions. Yellow background: net zero CO₂ emissions (potentially). Red background: net positive CO₂ emissions

The Intergovernmental Panel on Climate Change (IPCC) anticipates that the aim of limiting global warming to an average of 2°C, which corresponds to a CO_2 concentration of less than 450 ppm, can only be reached by wide-spread deployment of carbon capture and storage [17]. In addition, most scenarios simulated by the IPCC assume negative emission technologies such as BECCS to be deployed in the second half of the century. The potential for BECCS is estimated to equal negative CO_2 emissions of about 10 Gt/y. The climate mitigation cost in scenarios prohibiting the use of CCS is 138% higher than in the base case [2]

As the CO_2 stream to be stored in CCS has to be rather pure, the technologies used for CO_2 capture typically use a gas separation step: in oxyfuel processes, O_2 is extracted from air. In a subsequent step, the fuel is burnt with a mixture of O_2 and recirculated CO_2 to form exhaust gas ideally consisting of mainly CO_2 and water. In post- and pre-combustion processes, CO_2 is separated from the exhaust gas or the product gas of a preceding gasification process, respectively. As gas separation is inevitably associated with an energy penalty, all three technologies suffer from considerable losses in overall process efficiency. This energy penalty equals the minimum separation work, which for ideal gases can be calculated from the entropy of mixing:

$$W_{sep,min} = T \cdot \Delta S_{irr,mix} = T \cdot \sum n_i \cdot \ln x_i \qquad\qquad \textbf{(1)}$$

Mixing between CO_2 and nitrogen from air does not take place in CLC, resulting in a mixing entropy – and thus a thermodynamic separation work – equal to zero.

1.3 Chemical Looping Combustion

Within CCS, chemical looping combustion (CLC) represents a capture technology aimed at avoiding the above-mentioned energy penalty in the combustion of gaseous, liquid or solid fuels. In chemical looping, fuel and air are never mixed, eliminating the need for gas separation and thus reducing the separation work in equation (1) to zero. Instead, oxygen is transferred to the fuel by a solid oxygen carrier, typically a metal oxide. The concept can be realized using two interconnected fluidized bed reactors to ensure good heat and mass transfer. In the air reactor, the oxygen carrier particles are oxidized, after which they are transported to the fuel reactor, reduced by the fuel and transported back to the air reactor. Fig. 5 shows a schematic drawing of the process.
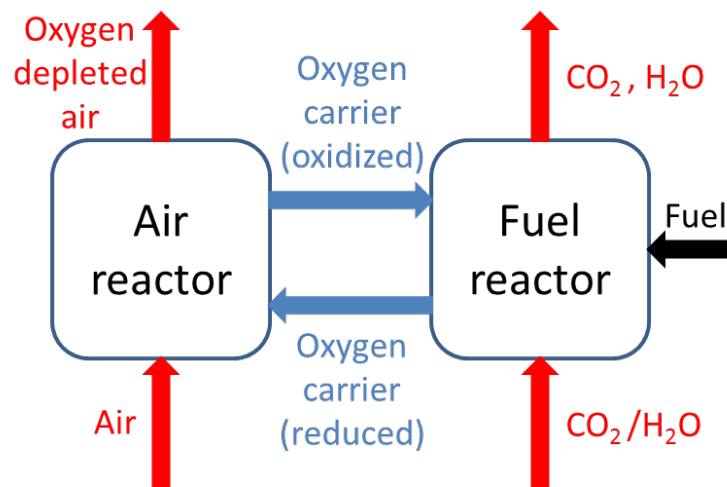
Fig. 5: Schematic of the CLC process for solid fuels

The first prototype reactors built were operated with gaseous fuels. However, focus has shifted towards solid fuels in the recent years.

The concept of solid-fuel CLC was first outlined by Lewis et al. [19]. Fifty years later, new studies emerged [20-22]. Leion et al. investigated the process in a bench-scale reactor, e.g. [23-25]. Lyngfelt recently presented a review on chemical looping combustion with solid fuels [26].

While gaseous fuels can be used in the CLC process right away, solid fuels have to be gasified by steam or CO_2 first. Fuel devolatilization and gasification are carried out in the same reactor as the reaction of these gases with the oxygen carrier. The gaseous volatiles and gasification products react with the oxygen carrier to form CO_2, H_2O and, if a sulphurous fuel is burnt, SO_2. It has been

shown that the presence of an oxygen carrier can increase the rate of gasification [25]. Equations (2) - (7) describe the principle of solid fuel gasification and subsequent chemical looping combustion:

Solid fuel → char (C) + tar + gas (H_2, CO, CO_2, CH_4, C_xH_y) **(2)**

$C + H_2O → CO + H_2$ **(3)**

$C + CO_2 → 2 CO$ **(4)**
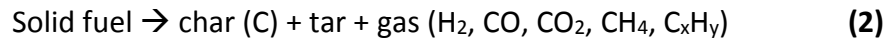
Reaction of volatiles and gasification products with oxygen carrier particles:

$Me_xO_y + H_2 → Me_xO_{y-1} + H_2O$, **(5)**

$Me_xO_y + CO → Me_xO_{y-1} + CO_2$, **(6)**

$4 Me_xO_y + CH_4 → 4 Me_xO_{y-1} + CO_2 + 2 H_2O$, **(7)**
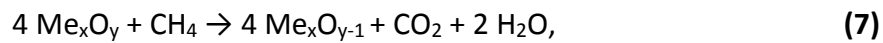
where methane represents all hydrocarbons released during devolatilization.

Gasification is a comparably slow reaction, which can lead to losses of unconverted char to the air reactor or fuel reactor exhaust. A possible solution for that problem is chemical looping with oxygen uncoupling (CLOU). In that concept, the oxygen carrier releases gaseous oxygen in the fuel reactor rather than merely transporting it in a chemically bound form [27]. In this case, a part of the solid fuel can react with gaseous oxygen without the need of gasification, which might facilitate the conversion of solid fuel especially in conditions with poor gas-solids mixing.

1.4 Status of Oxygen Carrier Development

The choice of oxygen carrier material is crucial to process performance. Potential materials have to meet a series of requirements:

- Sufficient oxidation and reduction rates, which are decisive for the needed amount of oxygen carrier material and reactor size
- Environmental benignity and non-toxicity
- Mechanical and chemical durability to minimize the need for material make-up
- Compatibility with possible fuel impurities
- Good fluidizability
- Low cost

The last point is especially important in chemical looping combustion of ash-containing solid fuels, in which oxygen carrier material will be continuously lost in ash separation.

In general, two major pathways can be followed in the choice of oxygen carrier materials:

1) Use of manufactured particles
2) Use of non-manufactured materials, e.g. natural ores or waste materials

While manufactured particles offer the possibility to be tailored to the specific use intended, which can result in better process performance, natural materials are cheaper. The gain in performance would thus have to be weighed against extra oxygen carrier cost in utility-size chemical looping units. Besides the choice between natural or manufactured materials, the chemical composition of the oxygen carrier is also important. According to thermodynamic analyses [28], oxides of nickel, iron, copper and manganese are feasible base materials for oxygen carriers.

To date, more than 3000 hours of continuous chemical looping operation with solid fuels has been reported , most of it with ilmenite, a naturally occurring iron-titanium material, as oxygen carrier. Ilmenite was chosen due to its comparably low cost, mechanical durability and non-toxicity [29-36] and has become the state-of-the-art oxygen carrier material [37]. When used with solid fuels, full gas conversion could not be reached with ilmenite, however. The material does not have considerable CLOU properties, either, which makes a gasification step necessary. Other iron oxides have been tested as well with varying results [38-40].

The limitations of known oxygen carriers have spurred the search for alternatives. Copper oxides possess CLOU properties and show good reactivity [41]. Experiments with biomass fuels and an oxygen carrier based on copper have been conducted by Adánez-Rubio et.al. [42]. More recently, the same group investigated a synthetic Cu-Mn oxygen carrier with different biomass fuels [43]. However, copper is an expensive raw material and the mechanical stability of copper-based oxygen carriers is uncertain [44, 45].

As a more cost-efficient alternative, manganese materials have been identified. Manganese oxide can release gaseous oxygen as well, but the use of pure manganese oxide is limited by slow re-oxidation and a low equilibrium temperature [27]. On the other hand, the combination of manganese with other metals can change these properties [46]. Combined oxides of manganese with iron, nickel, calcium, silicon, copper and magnesium have been tested previously, e.g. [47-50]. In combination with calcium, manganese can form a perovskite structure with the unit cell formula $ABO_{3-\delta}$, in which A is a larger and B a smaller cation. δ describes the degree of oxygen deficiency, which is zero for a perfect perovskite and depends on temperature, pressure and oxygen concentration in the surroundings. The possibility to change the oxygen content in the material by changing these parameters provides oxygen release properties and makes perovskites well suited as oxygen carriers.

Manufactured calcium manganate perovskites have proven to be resistant to mechanical wear in jet-cup attrition tests [51]. Taking up the promising work which has been done with these oxygen

carriers in combination with gaseous fuels previously [52, 53], papers I and II investigate their performance when used with solid fuels. In addition, paper II analyses the sulphur tolerance of the oxygen carrier.

In an attempt to find an oxygen carrier with similar gas conversion properties and durability as calcium manganate, but with higher sulphur resistance, combined oxides of manganese and silicon have moved into focus. These materials feature both favourable thermodynamic properties, sulphur tolerance and potentially low cost [54]. Hanning et al. [55] found that adding titanium to the matrix of a manganese silicon oxygen carrier can increase its mechanical durability. The same oxygen carrier was used in paper IV.

As mentioned above, ores can be used as a potentially cost-effective alternative to manufactured particles. Manganese ores typically have a high manganese content and are both cheap and abundant. The possibility of using manganese ores as oxygen carriers has been documented before: Sundqvist et al. [56] found that the rate of gas conversion could be increased by a factor 2.7 to 6 compared to ilmenite. Linderholm et al. [57] essentially halved the amount of unconverted gases leaving the fuel reactor by using a mixture of ilmenite and manganese ore in a 100 kW chemical looping combustor. On the other hand, some manganese materials have proven to be more prone to attrition than ilmenite [58]. To date, the database on operational experience with manganese ores is thin: apart from the work done at Chalmers, Sozinho et al. [59] performed experiments with a manganese-ore based oxygen carrier and Xu et al. [60] used manganese ore as support for impregnation with a copper solution. More recently, Pikkarainen et al. [61] conducted experiments with Braunite, a mineral sometimes used as manganese ore, and found an increase in performance as compared to ilmenite.

1.5 Aim of Study

The objective of this work is to investigate the feasibility of using manganese-based oxygen carriers in continuous solid-fuel chemical looping combustion, both by testing new materials and materials that have shown promising results in bench-scale reactors or with gaseous fuels previously. The experiments are carried out in 10 kW and 100 kW chemical looping reactors as described in section 2, with a focus on process performance and particle integrity. Both manufactured (papers I, II and IV) and natural materials (papers III and V) are investigated and a comparison as to the cost and benefits of either material category is conducted.

Establishing several working alternatives for oxygen carrier materials could greatly improve the robustness of the technology with respect to material price changes and availability issues, the long-term objective is to find a range of different materials which can be used in utility-scale operation. To be considered as candidates for up-scaling, the oxygen carriers have to show good reactivity towards both volatiles and gasification products (CO and H_2). Volatiles conversion has

been identified as an issue in CLC before [62] and is therefore a research focus in papers IV and V.

As to the lifetime of the particles, crushing strength and attrition have oftentimes been chosen as indicators for the durability of the particles in previous studies. However, only a limited correlation with the actual lifetime determined in continuous CLC units could be shown [63]. Although labour-intensive, the only method believed to give a relevant estimation of particle lifetime in a chemical looping unit is a mass balance over the fines produced in a system in operation. This is because attrition is often a result of both chemical and mechanical stresses. A substantial part of the work done in papers IV and V is therefore dedicated to closing the particle mass balances and assessing the lifetime and the uncertainties tied to its calculation, both of which are considered to be crucial factors in technology scale-up and the running cost of potential full-scale units.

2. Experimental Setup

The experiments in papers I-IV were conducted in a 10 kW dual fluidized bed unit. The description of this unit is largely adopted from paper III. The 100 kW unit was described in paper V.

2.1 10 kW Unit

The reactor is based on interconnected fluidized-bed technology. In the riser, which constitutes the upper part of the air reactor, high gas flows in combination with a small cross-section area ensure high gas velocities which provide the driving force for the circulation. The entrained oxygen carrier particles enter a cyclone, where they are separated from the air flow and fall into the fuel reactor via a loop seal to avoid gas mixing, see Fig. 6.
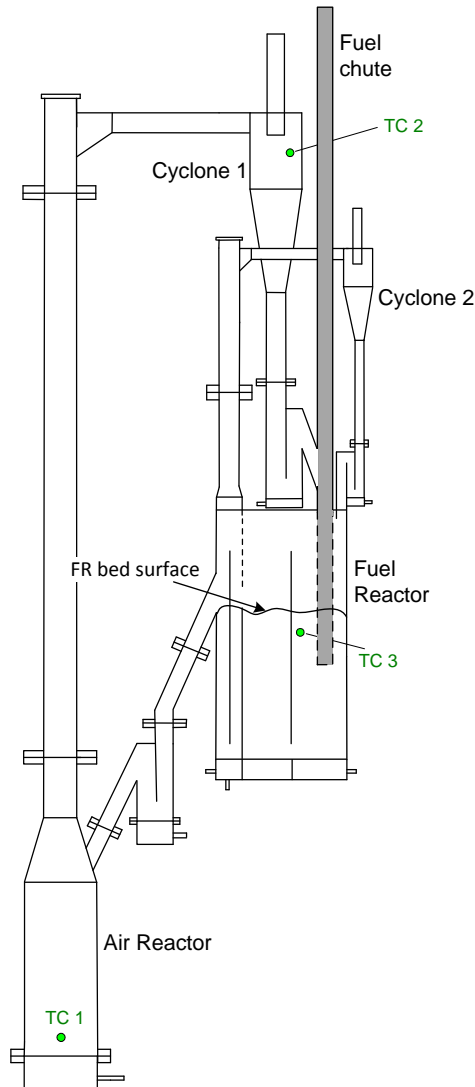

Fig. 6: 10 kW solid fuel chemical looping combustor. TC 1-3 mark thermocouple positions

The fuel reactor is designed as a bubbling bed and consists of several parts: in the main section, fuel is oxidized to CO_2 and H_2O. The char remaining after devolatilization is gasified followed by oxidation of the gasification products by the oxygen carrier. The main section is usually fluidized with steam. The particles are forced to pass under a vertical wall. The left section of the fuel reactor is fluidized by nitrogen. By increasing the fluidization velocity, char and oxygen carrier particles are separated due to their different densities. The lighter char particles are entrained and returned to the fuel reactor via a small loop seal, whereas the heavier reduced oxygen carrier particles continue to the air reactor.

Fuel is introduced into the fuel-reactor bed via a coal screw and a fuel chute. The operating temperature is measured via three thermocouples located in the air reactor, fuel reactor and air reactor cyclone. Fluidization behaviour, solids circulation and inventory can be estimated from numerous pressure measurements. The exhaust gas streams from both air and fuel reactor are passively cooled before entering filter bags (air reactor exhaust) or a water seal (fuel reactor exhaust). The water seal is used both to collect condensate from fuel conversion and steam fluidization and to impose a hydrostatic pressure on the fuel reactor exhaust, thus creating a pressure difference between the outlets of the fuel reactor and air reactor. This is necessary to avoid inadequate pressure differences over the loop seals connecting the reactors.

A part of the exhaust gas streams is cooled, filtered for removal of fines, led through gas conditioning systems to condense remaining steam and then analysed by infrared- (CO, CO_2 and CH_4), thermal conductivity- (H_2) or paramagnetic analysers (O_2). Apart from that, gas samples can be withdrawn and analysed in detector tubes.

Before heat-up and operation with fuel, the 10 kW unit is filled with 15-20 kg of oxygen carrier particles. To maintain operating temperature, the unit is enclosed in an electrically heated furnace, which also is used to heat up the unit initially. During heat-up, all parts of the unit are fluidized by air before switching to steam-/nitrogen fluidization of the fuel reactor, the loop seals and the carbon stripper.

Previous operational experience in this unit has been achieved using ilmenite and manganese ore [29, 31, 58, 64-67].

2.2 100 kW Unit

A 2D and 3D drawing of the 100 kW unit are shown in Fig. 7.
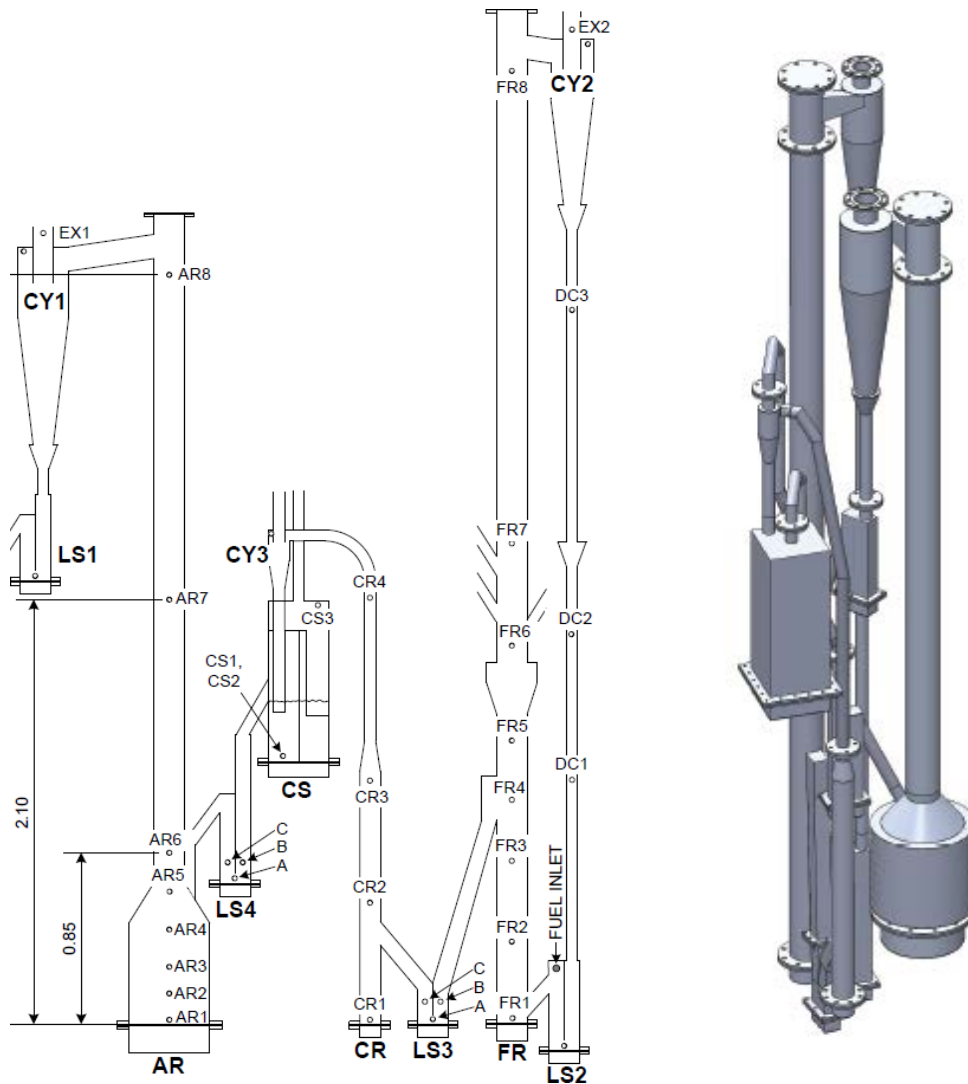
Fig. 7: 100 kW pilot, 2D and 3D drawings.

While the general principle – fluidized beds connected by loop seals – is the same as in the 10 kW unit, the 100 kW pilot design is more complex. The main differences are:

- **Separate carbon stripper**

In order to reduce carbon losses as compared to the 10 kW unit, a carbon stripper with considerably higher cross section in relation to the fuel input and increased residence time of the oxygen carrier was designed for the 100 kW reactor. In this, the influence of different variables such as gas velocity or fluidization agent can be studied. Also, the increased residence time allows for additional char gasification: Markström et al. [68] found a threefold increase of unconverted char entering the air reactor in experiments with bituminous coal and ilmenite when the carbon

stripper was fluidized with nitrogen instead of steam, demonstrating the effect of char gasification in the carbon stripper.

- **Intermediate riser between fuel reactor and carbon stripper**

The design of the unit is constrained by the height of the lab hall. With gravity as the only driving force for returning oxygen carrier particles to the air reactor, the fuel reactor would have needed to be higher than carbon stripper and air reactor. To achieve a fuel reactor height of about 5 metres, an additional circulation riser – denominated "CR" in Fig. 7– had to be included in the construction. Also, this solution enables the operator to change the solid inventory of the fuel reactor independent of the global solids circulation.

- **Fuel reactor fluidization regime**

As opposed to the 10 kW unit, the fuel reactor of the 100 kW unit is designed as a circulating fluidized bed, enabling potentially better contact between gas and oxygen carrier and thus a higher ability to convert volatiles and gasification products.

- **Steam fluidization of all reactor parts except air reactor**

The fuel reactor, all four loop seals, the carbon stripper and the circulation riser are fluidized by steam, whereas in the 10 kW unit, loop seals and carbon stripper are fluidized by nitrogen. As a result, some amount of char gasification might take place outside of the fuel reactor.

- **Post oxidation chamber (POC)**

The POC is located downstream of the fuel reactor exhaust outlet and consists of a well-insulated steel pipe with air injection at several points, see Fig. 8. The surplus oxygen added with the air flow oxidizes most of the unconverted gases and char particles in the exhaust stream. In an industrial size unit, the air injected would be replaced by pure oxygen from an air separation unit to avoid adding nitrogen to the exhaust gas before compression, transport and injection. The amount of pure oxygen needed to reach full conversion has an important impact on the total process cost, thus further emphasizing the importance of high gas conversion within the process.
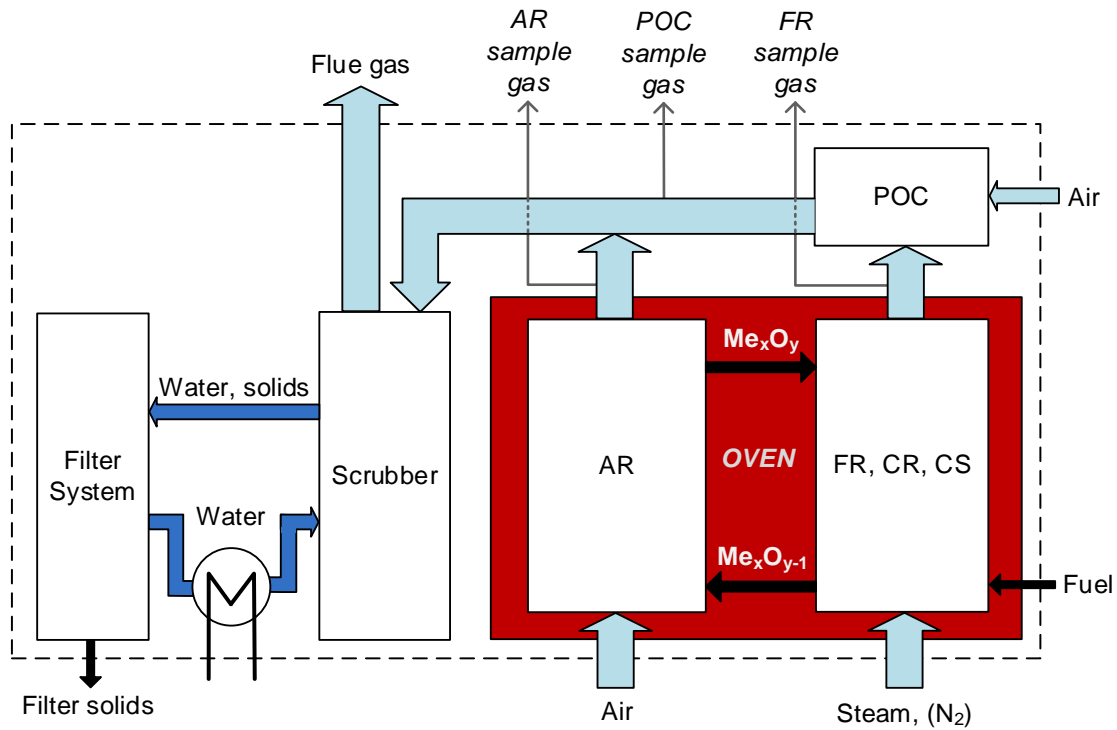
Fig. 8: 100 kW system, process scheme with main flows of gas (light blue arrows), solids (black) and water (dark blue) [69].

2.3 Oxygen Carriers

Six different oxygen carriers were investigated in the experiments, two manufactured materials and four ores, two of which consisted of sintered ore fines. The mean particle size was in the range of 150-200 μm.

The manufactured material used in papers I and II ($CaMn_{0.9}Mg_{0.1}O_{3-\delta}$) has CLOU properties and was produced by spray-drying a mixture of 46.8% Mn_3O_4, 50.5% $Ca(OH)_2$ and 2.7% MgO followed by a four-hour calcination period at 1300°C. The natural materials ("Mangagran", "Mesa" and "Sinfin") used in paper III were chosen with respect to chemical composition and mechanical properties such as crushing strength to cover a wide range of potential oxygen carrier materials. The manganese content was between 40 and 66%. All three materials were crushed and calcined at 950˚C for 24 hours.

In paper IV, a spray-dried manganese-silicon-titanium oxygen carrier was used to investigate whether the sensitivity to sulphur poisoning experienced in paper II could be avoided. Calcination temperature for this material was 1100°C. Paper V is a comparative study, investigating a promising natural material in both the 10 kW and 100 kW reactor. The oxygen carrier used here ("Sibelco Calcined", SC) is a pre-calcined manganese ore.

2.4 Fuels

Wood char, pet coke and a mixture of both were used as fuels in papers I-III. The mixture was meant to simulate a sulphur content typically found in hard coal. The wood char is produced by subjecting wood chips of both hard- and softwood to 450°C for 8 h in the absence of oxygen. The as-received wood char has a size of approximately 5 mm, which is reduced to 200-1000 µm when the fuel is passed through the feeding screw. The pet coke has a mass-weighted mean diameter of 79 µm.

In papers IV and V, more fuels were tested in order to accommodate for fuel types with different physical and chemical properties, mainly sulphur and volatile contents. Table 1 shows composition and heating value of the fuels used.

Table 1. Composition of fuels: proximate and ultimate analyses.

Component	Swedish wood char	Pet coke	Coal, partly de-volatilized	Lignite	German wood char	Black pellets	Bitumin-ous coal	Comment
Fixed carbon	73.9	81.5	62.0	40.0	74.3	18.7	53.1	as received
Volatiles	16.7	10.0	29.1	45.0	15.9	74.2	29.4	as received
Moisture	3.9	8.0	2.7	11.0	4.2	6.9	11	as received
Ash	5.5	0.5	6.2	4.0	5.6	0.3	6.5	as received
C	86.9	88.8	77.9	66.9	83.3	53.5	78.3	maf
H	3.2	3.1	4.0	4.8	2.4	6.0	6.6	maf
O	9.5	0.5	9.5	22.8	7.8	40.3	12.7	maf
N	0.4	1.0	1.9	0.8	0.6	0.1	1.6	maf
S	0.03	6.6	0.6	0.8	0.02	0	0.8	maf
LHV (MJ/kg)	29.8	31.8	24.3	22.2	29.3	18.6	24.6	as received

maf: moisture and ash free

2.5 Data Evaluation

The performance of the materials is judged based upon two main characteristics: chemical and mechanical performance. While the chemical performance is measured by the conversion of fuel to combustible gases and finally to fully oxidized combustion products, the mechanical properties determine the average time an oxygen carrier particle can be used in the system without breaking down.

Oftentimes, the choice of oxygen carrier material is a trade-off between mechanical and chemical properties; materials offering high mechanical strength can be less reactive, e.g. due to lower internal particle surface, and vice versa. For manufactured materials, the properties can be fine-tuned by the adaption of sintering temperature and duration.

2.5.1 Conversion Performance

Unconverted fuel species can escape the fuel reactor in three different ways: as unconverted gas, as char particles to the air reactor or as elutriated char.

The unconverted gas species in the fuel reactor exhaust are made up of both volatile fuel compounds and gasification products. The *oxygen demand,*

$$\Omega_{OD} = \frac{0.5x_{CO,FR} + 2x_{CH_4,FR} + 0.5x_{H_2,FR}}{\Phi_0\left(x_{CO_2,FR} + x_{CO,FR} + x_{CH_4,FR}\right)} \qquad \textbf{(8)}$$

describes the fraction of oxygen which after conversion in the fuel reactor is lacking to achieve full conversion and would have to be added in an oxygen polishing step. In this definition, Φ_0 is the molar ratio of oxygen needed to oxidize the fuel to moles of carbon contained in the fuel [29]. The conversion of combustible gases in the fuel reactor can be defined as *gas conversion* and calculated to

$$\eta_{gas} = 1 - \Omega_{OD} \qquad \textbf{(9)}$$

Both oxygen carrier and unconverted fuel particles move in a continuous flow from the fuel reactor to the air reactor. Some char particles will therefore escape the fuel reactor before they can be fully gasified. These particles will eventually be oxidized by air in the air reactor and thus evade the carbon capture process. The *oxide oxygen efficiency* is the ratio of oxygen used for reoxidation of the oxygen carrier to the total oxygen consumption in the air reactor:

$$\eta_{OO} = \frac{0.21 - x_{O_2,AR} - x_{CO_2,AR}}{0.21 - x_{O_2,AR} - 0.21x_{CO_2,AR}} \qquad \textbf{(10)}$$

A precise calculation of that performance indicator is possible because it only depends on gas concentrations. Because the oxygen not used for oxidizing the oxygen carrier is used for oxidizing the char, η_{OO} provides a good estimation of the carbon capture efficiency. This is further explained in [32]. Therefore, η_{OO} will be referred to as *carbon capture efficiency* in the following.

A certain portion of the fuel will be lost as char particles elutriated to the fuel reactor chimney. This loss of unconverted fuel can be described by the *solid fuel conversion,* defined as the sum of all carbon in the form of gaseous compounds leaving the fuel and air reactor divided by the total carbon added with the fuel.

$$\eta_{SF} = \frac{F_{C,FR} + F_{C,AR}}{F_{C,FUEL}} \qquad \textbf{(11)}$$

$F_{C,FR}$ and $F_{C,AR}$ denote the molar flows of carbon from the fuel reactor and air reactor, and $F_{C,FR}$ the flow of carbon to the reactor system with the added fuel. The 10 kW reactor is mainly designed to evaluate gas conversion and carbon capture efficiency. The cyclone efficiency is poor and the low fuel reactor height in the 10 kW unit results in considerably shorter residence times for fuel (char) particles entrained from the bed than in industrial size units. In the 100 kW unit, most of the elutriated char is burned in the POC. If the solid fuel conversion for the core CLC process, i.e. without any influence POC, is to be considered, the air flow to the POC has to be switched off during a period of time. In the experiments conducted in paper V, this was not done because focus was mainly on gas conversion and lifetime assessment.

Anyhow, previous experiments in the 100 kW unit have shown carbon elutriation rates of around 35% with ilmenite [70], which could be reduced to 20% with a mixture of ilmenite and manganese ore and further to 7% using a sintered manganese oxygen carrier. For industrial size units, Lyngfelt and Leckner [71] assume the char conversion to be 97% in the fuel reactor of a 1000 MW unit, with the remainder reacting in the post-oxidation chamber.

2.5.2 Solids circulation

Knowing the amount of solids circulating through the system can give valuable information about the amount of oxygen available for fuel conversion in the fuel reactor, which in turn influences conversion performance and the degree of oxygen carrier conversion.

In the 10 kW unit, the *circulation index, CI,* is used as a measure of solids circulation in the reactor. *CI* as defined in [64] is based on measurements of the pressure drop over the riser and the air reactor temperature and gas flow and is used to investigate the relationship between solids circulation and conversion performance.

$$CI = \Delta p_{riser} \cdot F_{AR} \cdot \frac{T_{AR} + 273}{273} \qquad \textbf{(12)}$$

In the 100 kW unit, Linderholm et al. [72] went one step further and determined the actual mass flow of particles through the system to be:

$$\dot{m}_{OC} = 6.6 + 0.057 \cdot \frac{A_c}{g} \cdot \frac{\Delta p_{riser}}{\Delta h} \cdot (u_0 - u_t) \qquad \textbf{(13)}$$

In this equation, A_c is the cross section of the air reactor riser, g is gravity, Δh the riser height and $u_0 - u_t$ the difference between superficial and terminal velocity in the riser.

2.5.3 Lifetime of the Oxygen Carrier

During operation, some of the oxygen carrier particles break into smaller pieces. Repeated oxidation and reduction processes with the associated phase changes in combination with high-velocity collisions with the bottom plate and cyclone walls demand a high attrition resistance of the oxygen carrier particles. The fragments of particles below a certain diameter are called *fines.* The production of fines, Δm_{fines}, during a certain period of time, Δt, can be used to calculate the lifetime L_f:

$$L_f = \frac{\Delta m_{fines}}{\Delta t} \cdot \frac{1}{m_I} \qquad\qquad \textbf{(14)}$$

with m_I being the total solids inventory. The corresponding oxygen carrier lifetime can be expressed as:

$$t_{life} = \frac{1}{L_f} \qquad\qquad \textbf{(15)}$$

It should be noted that the oxygen carrier in solid fuel chemical looping combustion is also exposed to ash fouling which may cause loss in reactivity and ultimately particle deactivation. The rate of ash fouling is not known, but should depend on the fuel used. It cannot be ruled out that fouling leading to significant loss of reactivity occurs well before $1/L_f$ is reached, in which case the lifetime of the carrier is governed not by the attrition rate but by the rate of fouling.

Spurred by experience and taking into account operational considerations, the method for fines removal and –registration evolved over time; from a mostly qualitative estimation of the lifetime in paper I over a more systematized method based on wet-sieving in paper III to a rigorous global fines balance used in papers IV and V, the method grew more sophisticated and led to an increased knowledge on the different materials' long-term performance. Also, in papers IV and V the FR material was recycled after burning off char residues, eliminating the need for a make-up stream of fresh particles. It thus became possible to investigate long-term performance without the superposed influence of fresh particles. Due to operational reasons, the limit for the definition of *fines* was moved from 45 to 63 µm in papers IV and V.

2.5.4 Oxygen Carrier Conversion

The oxygen carrier material is cyclically reduced in the fuel reactor and oxidized in the air reactor, which entails a fluctuation in the mass of each particle. The degree of oxygen carrier conversion, ω, is then described by the ratio of actual mass and fully oxidized mass of a particle sample:

$$\omega = \frac{m}{m_{ox}} \leq 1 \qquad\qquad \textbf{(16)}$$

This quantity is impractical to measure, which is why this study instead uses the average oxygen carrier conversion on the fuel reactor, ω_{FR}, to express the degree of oxidation.

$$\omega_{FR} = \frac{\dot{m}_{OC}}{\dot{m}_{OC} + \dot{m}_{ox,trp}} \qquad\qquad \textbf{(17)}$$

$\dot{m}_{OC}$ is the flow of oxygen carrier as defined in equation (13) and $\dot{m}_{ox,trp}$ the mass flow of oxygen used to oxidize the particles in the air reactor. ω_{FR} can thus be calculated solely from gas concentrations and pressure drops without the need for solids sampling and is a useful indicator for the determination of chemical stresses the material has to endure. In this work, oxygen carrier conversion was correlated with particle lifetime only for the 100 kW experiments.

3. Results

The most important results from papers I-V with a focus on conversion performance and particle lifetime will be presented in this chapter.

3.1 Experiments with Calcium Manganate and Biomass Fuel (paper I)

$CaMn_{0.9}Mg_{0.1}O_{3-\delta}$ was operated for 37 hours with a fuel power of 3.5-7.5 kW_{th}, yielding a solids inventory of 770 to 1660 kg/MW_{th}. The standard fuel reactor operating temperature was set to about 970°C, with low temperature tests being performed as parameter studies. Stable operation throughout a long period of time was reached in most cases.

Fig. 9 shows a compilation of the average values of Ω_{OD} and η_{OO} for all tests done at $T_{FR} \approx 970$°C.
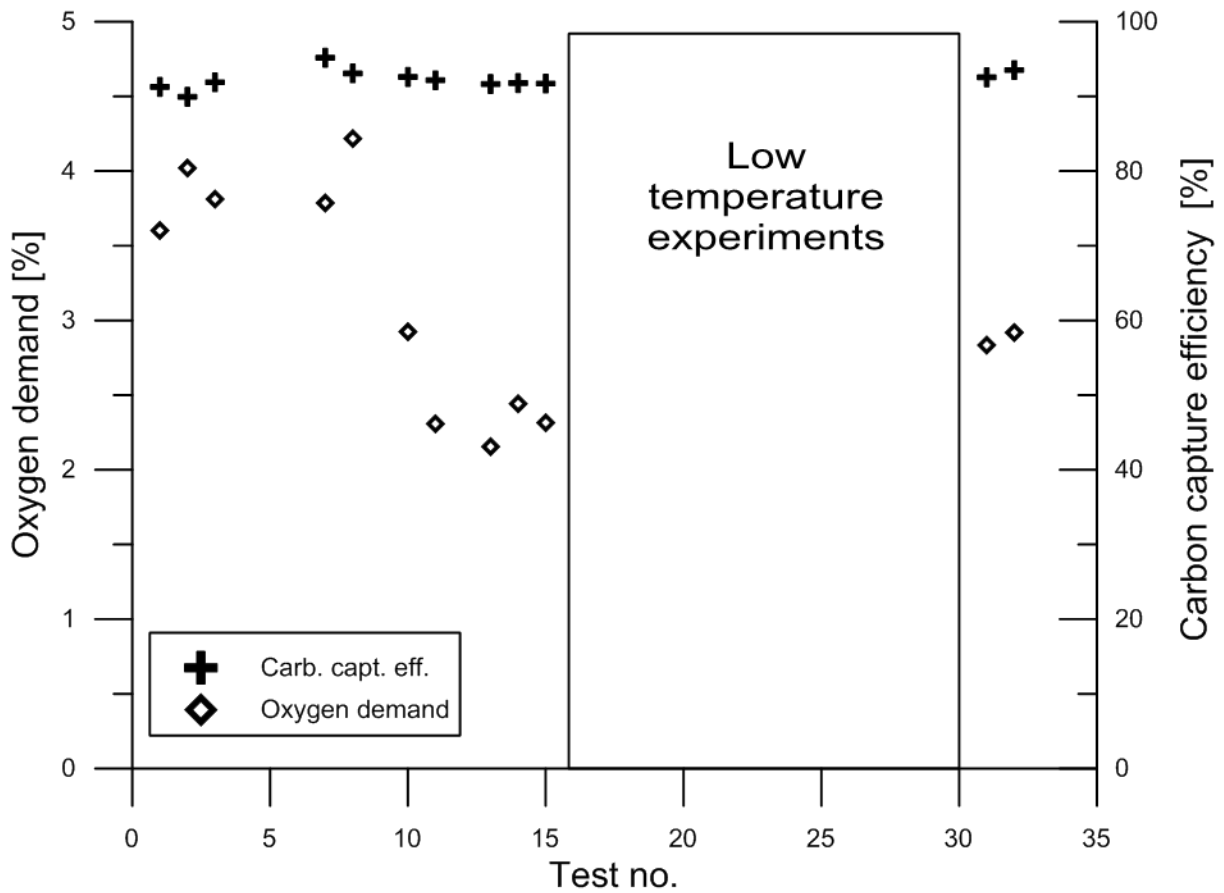

Fig. 9: *Average values for Ω_{OD} and η_{OO} for all experiments done at $T_{FR} \approx 970$°C*

An oxygen demand between 2.1 and 4.3% was reached while the carbon capture efficiency was in the range of 90-95.2%. Ilmenite has not been tested with the same fuel in the same unit. However, Linderholm et al. [62] used the same fuel and ilmenite as an oxygen carrier in a 100 kW

chemical looping combustor, which gave an oxygen demand of 4.7-10% and a carbon capture efficiency of 93-97%. The same authors also found that the performance of the 100 kW unit is generally superior to that of the 10 kW unit. Combined, these findings indicate that $CaMn_{0.9}Mg_{0.1}O_{3-\delta}$ offers conversion performance superior to that of ilmenite.

In theory, the oxygen carrier should release more oxygen at higher temperatures [73], resulting in higher conversion. Fig. 10 shows the system performance as a function of temperature.
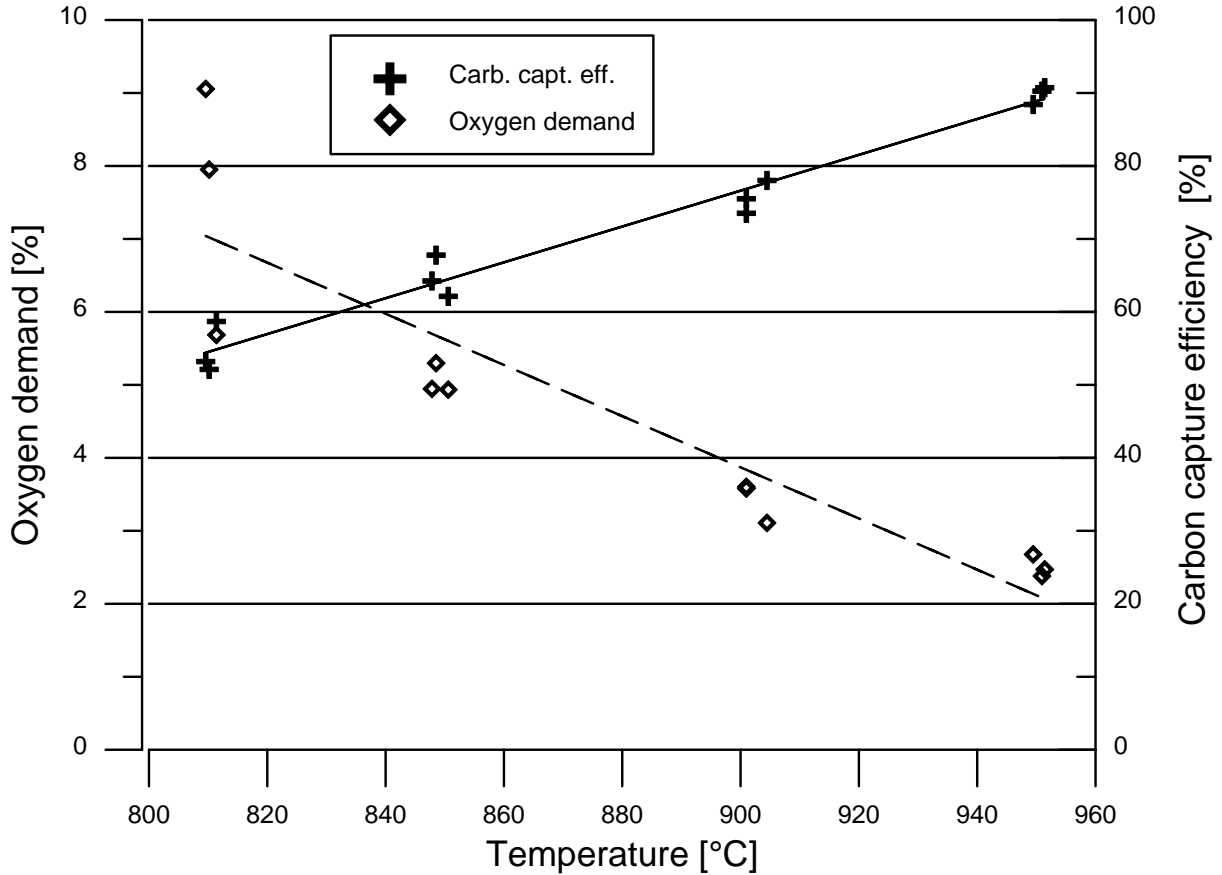

Fig. 10: *Average values for Ω_{OD} and η_{OO} at low temperatures (T<970°C)*

Different fuel feeding rates were examined as well and shown to have a considerable effect only at low temperatures. Overall, higher fuel reactor temperatures proved to be beneficial for process performance, both with regard to oxygen demand and carbon capture efficiency.

The air reactor gas flow is one of the main drivers for solids circulation in the system as stated in [64]. Fig. 11 shows the results of an experiment in which the air reactor flow was varied to determine the influence of solids circulation on the system performance. The fuel reactor temperature ranged from 917 to 928°C.
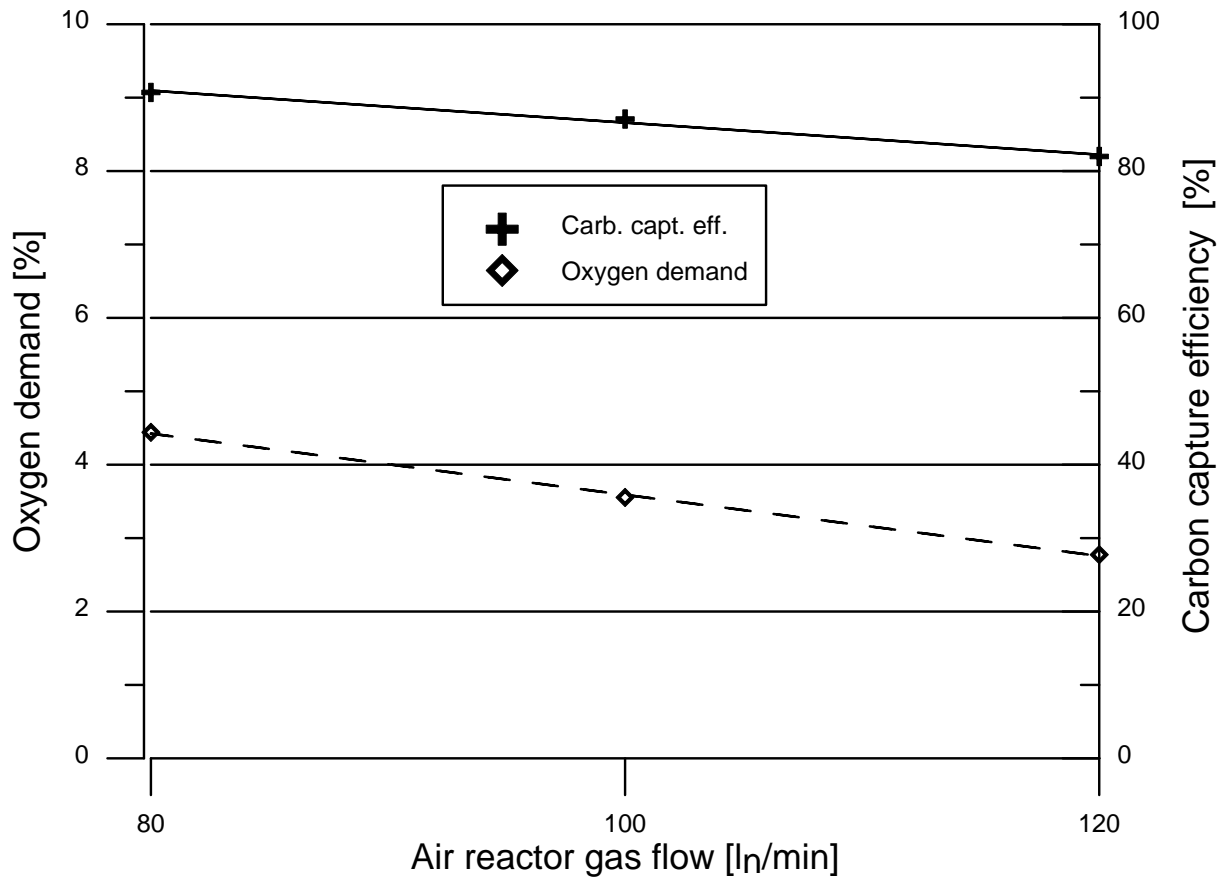
Fig. 11: *Average values for Ω_{OD} and η_{OO} while varying the air reactor gas flow*

Both oxygen demand and carbon capture efficiency decreased, an outcome which was expected: while a higher solids circulation leads to a thermodynamically favourable situation with more oxygen available, it also results in shorter solids residence time in the fuel reactor, giving the fuel particles less time to gasify before re-entering the air reactor.

The oxygen releasing properties of the material could be investigated prior to each experimental campaign. Once the operating temperature had been reached, fluidization of the fuel reactor and loop seals was switched to nitrogen. An average oxygen concentration of 2.5-3.8% was measured for fuel reactor temperatures of 950-970°C, which confirms previous experiments with the same type of oxygen carrier [52, 74]. Also, one experiment with fuel addition and nitrogen fluidization in the fuel reactor was conducted to investigate whether operation without steam gasification was possible, see Fig. 12. When fluidizing with nitrogen, i.e. in the absence of steam gasification, pure CLOU operation was possible. In these conditions, the carbon capture efficiency decreased due to slower char conversion. On the other hand, this resulted in a decrease of the total amount of combustible gases present in the fuel reactor while the available amount of oxygen remained constant, which in turn effectively increased the oxygen-carrier-to-fuel ratio and gave a lower oxygen demand.
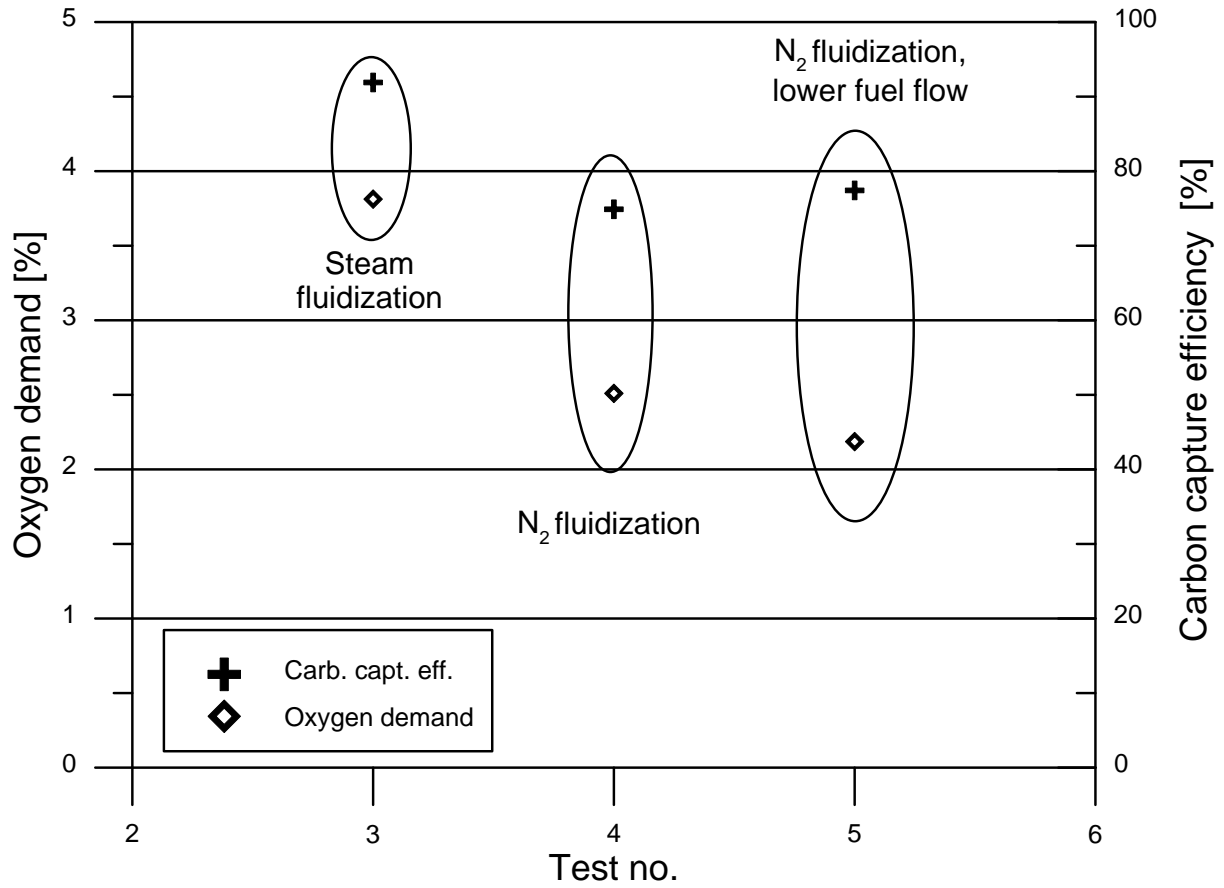
Fig. 12: Ω_{OD} and η_{OO} as a function of fuel reactor fluidization gas and fuel feeding speed

The oxygen carrier was easily fluidized and did not form hard agglomerations. The estimation of particle lifetime was complicated by the fact that the exact amount of ash and char in the elutriated particles was unknown and could only be determined in post-operation sample analysis. The results suggested that particle fines production more or less stopped toward the end of the experimental series. This indicates a high potential oxygen carrier lifetime, which is in line with earlier findings from a similar unit using gaseous fuels [52].

3.2 Experiments with Calcium Manganate and Sulphurous Fuels (paper II)

When using $CaMn_{0.9}Mg_{0.1}O_{3-\delta}$ with sulphurous fuels, the calcium cation might bond with SO_2 from the combustion process to form $CaSO_4$, which could inactivate the oxygen carrier [75-78]. Higher temperatures favour the formation of CaO at certain SO_2 and O_2 partial pressures. Assuming a similar behaviour for $CaMn_{0.9}Mg_{0.1}O_{3-\delta}$ as for CaO [74], high temperatures should allow for combustion of sulphurous fuels without $CaSO_4$ formation and the regeneration of $CaSO_4$ already formed.

29 hours of experiments with sulphur-containing fuels were conducted followed by a test with low-sulphur biochar to investigate the possibility of oxygen carrier regeneration.

When using a mix of 80 mass-% wood char and 20 mass-% petroleum coke, an oxygen demand of little more than 5% could be reached at standard conditions. The lowest oxygen demand with pure pet coke was around 7.7%, which can be compared to an oxygen demand of around 2% for pure biochar as described in paper I. The difference in gas conversion is believed to originate from the reactivity of the char, not the sulphur content: wood char has previously been shown to be more reactive than pet coke char [62]. Also, char gasification products are converted to a higher extent than volatiles due to better gas-solids mixing. Consequently, a fuel with low volatile content and high char reactivity such as wood char is expected to show good gas conversion. Fig. 13 shows oxygen demand and carbon capture efficiency for all tests at standard conditions.

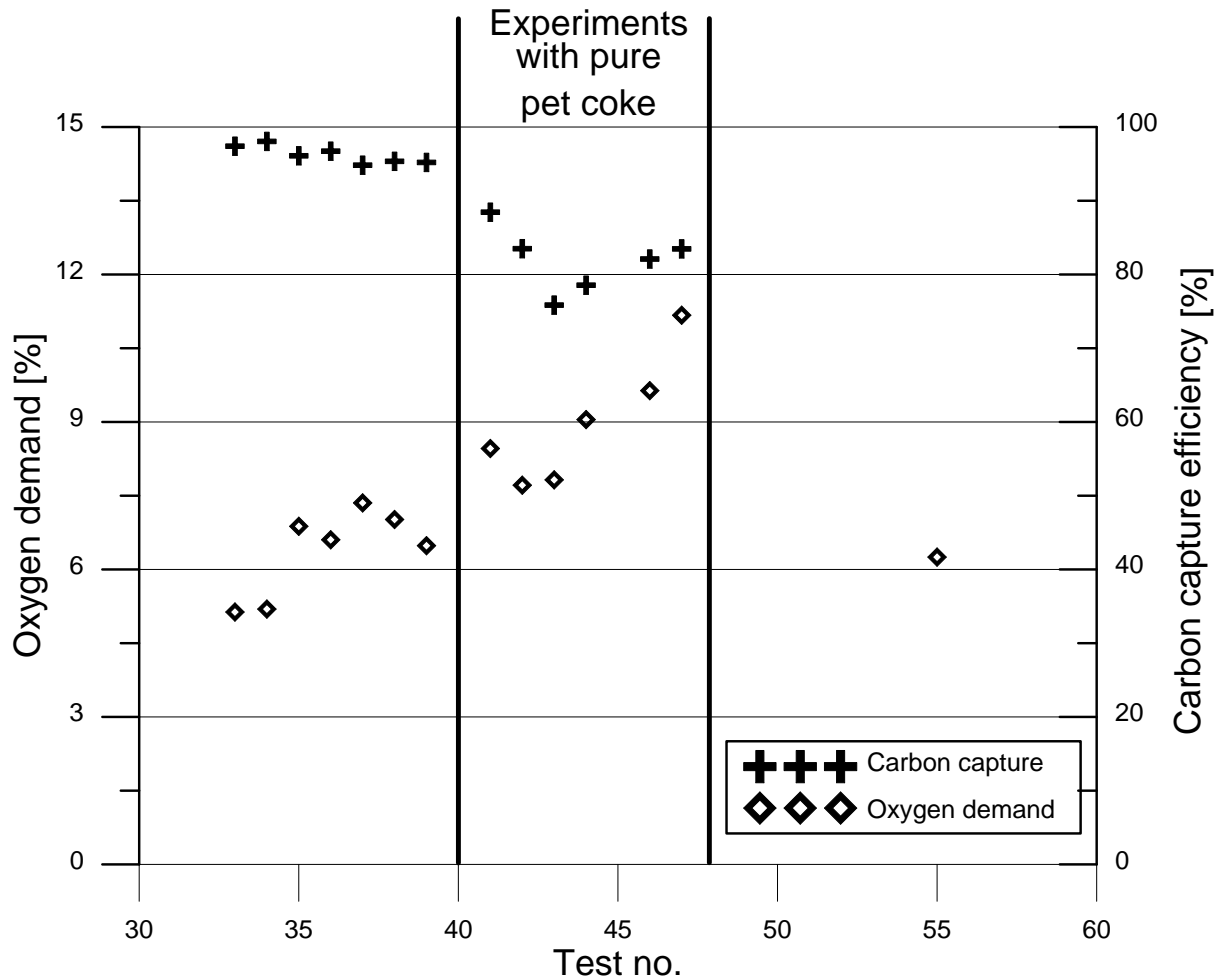Fig. 13: Average values for Ω_{OD} and η_{OO} at standard conditions

During the experiments with pet coke, system performance worsened with time. The observed levels of sulphurous gas species in the fuel reactor exhaust gases were low, which indicated

25

sulphur accumulation and poisoning of the oxygen carrier. After oxygen carrier regeneration (test no. 55), the oxygen demand decreased approximately to the base level. In this test, carbon capture efficiency could not be calculated due to a gas leakage.

The regeneration test was conducted at fuel reactor temperatures of 970-1030°C using low-sulphur biochar. During the experiment, the sulphur content in the exhaust gases was measured every five minutes, see Fig. 14.
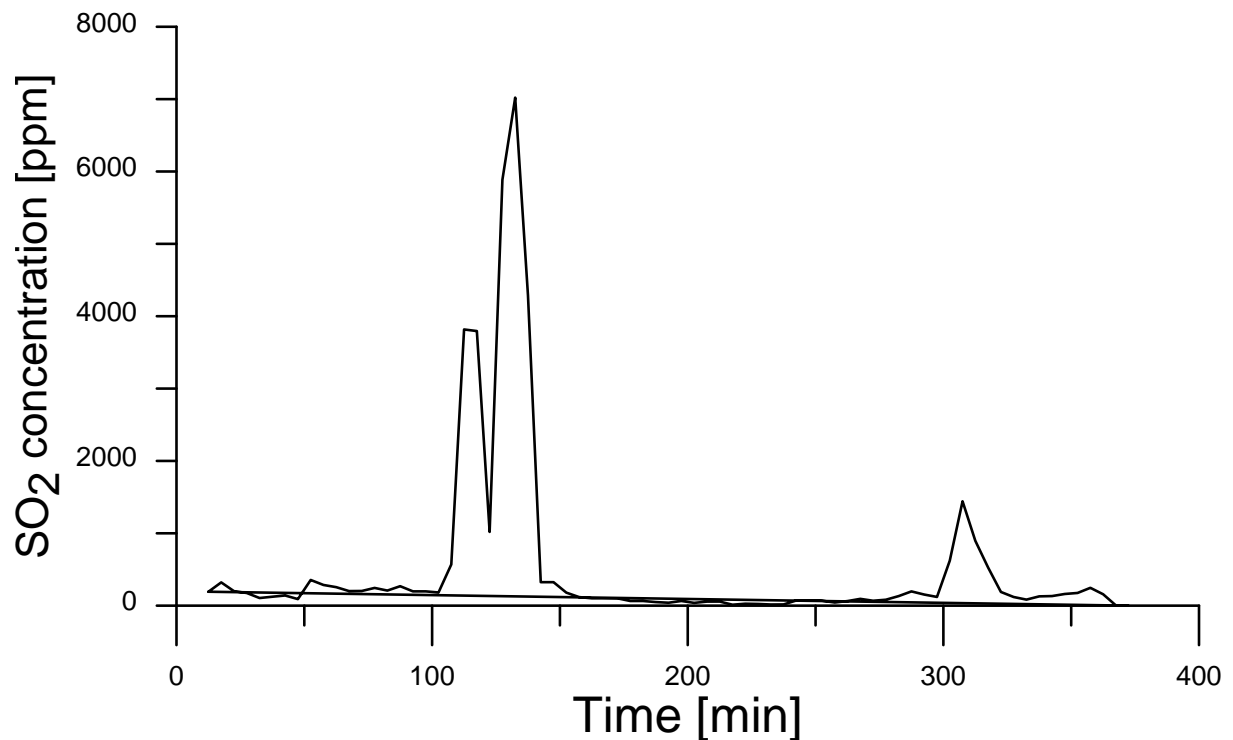
Fig. 14: SO₂ concentration during regeneration experiment (tests 48-53). Measurements were made every five minutes

After around 100 minutes, SO$_2$ levels increased to more than 7000 ppm although the fuel used contained almost no sulphur. The highest levels were reached before the fuel reactor temperature was increased to 1030°C at t=180 min, which could mean that the absence of sulphur in the fuel rather than the high temperature caused the sulphur release. Analyses of particle samples taken throughout all experiments confirmed that sulphur was first accumulated in the oxygen carrier during the experiments with sulphurous fuel, and then released during the regeneration test.

Although regeneration of the oxygen carrier is possible according to these results, it can be discussed if and to which extent the need for regular regeneration cycles, i.e. changes in operating temperature and fuel type, would impede the use of the material in larger scale.

3.3 Use of Natural Manganese Materials (paper III)

Three materials ("Sinfin", "Mangagran" and "Mesa") were tested for 14.6 h, 16 h and 11.5 h, respectively. Besides wood char, pet coke was used as fuel in the Sinfin tests to compare the oxygen carrier's performance with ilmenite, which had been tested with the same fuel in the same unit [31, 58, 79].

Fig. 15 shows average values for oxygen demand and carbon capture efficiency for all test periods with Sinfin.
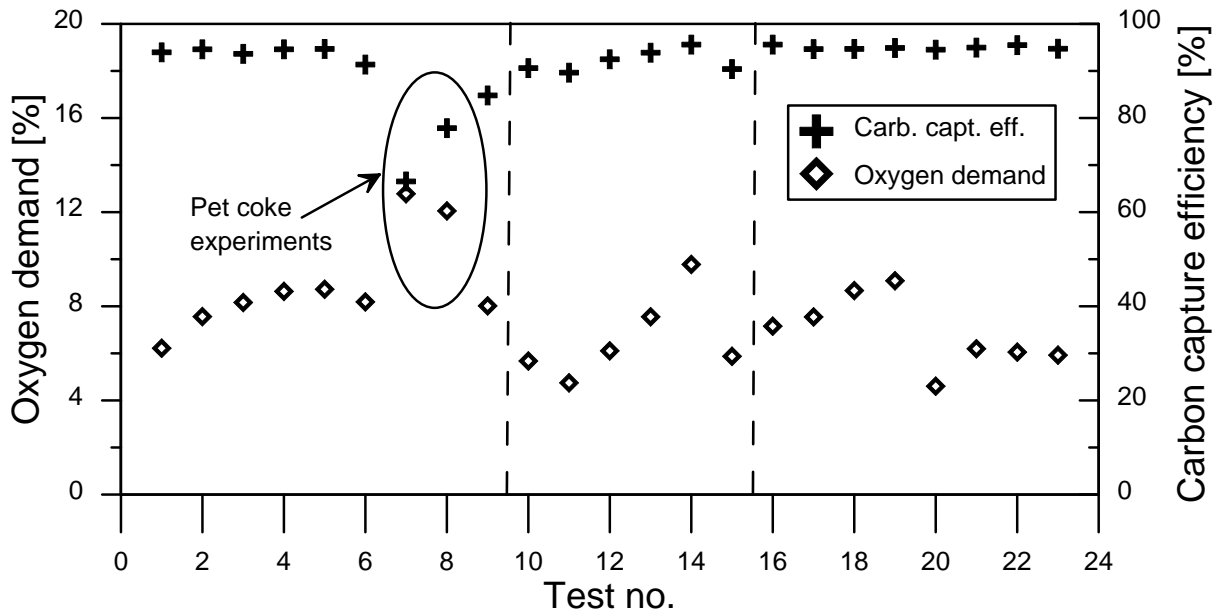
Fig. 15: Average values for oxygen demand and carbon capture for all Sinfin test periods.

In tests 7 and 8, pet coke was used as fuel. Experiments took place on three days, separated by vertical dashed lines in the diagram. After the first two test days and prior to test 17, fresh oxygen carrier material was added to the reactor to compensate for attrition losses. A clear correlation between higher solids inventory and better gas conversion, i.e. lower oxygen demand was observed, most likely caused by the increase in solids circulation associated with a higher solids inventory. Fig. 16 shows average values of oxygen demand and carbon capture efficiency in all test periods with Mangagran. Fig. 17 shows all tests with Mesa.
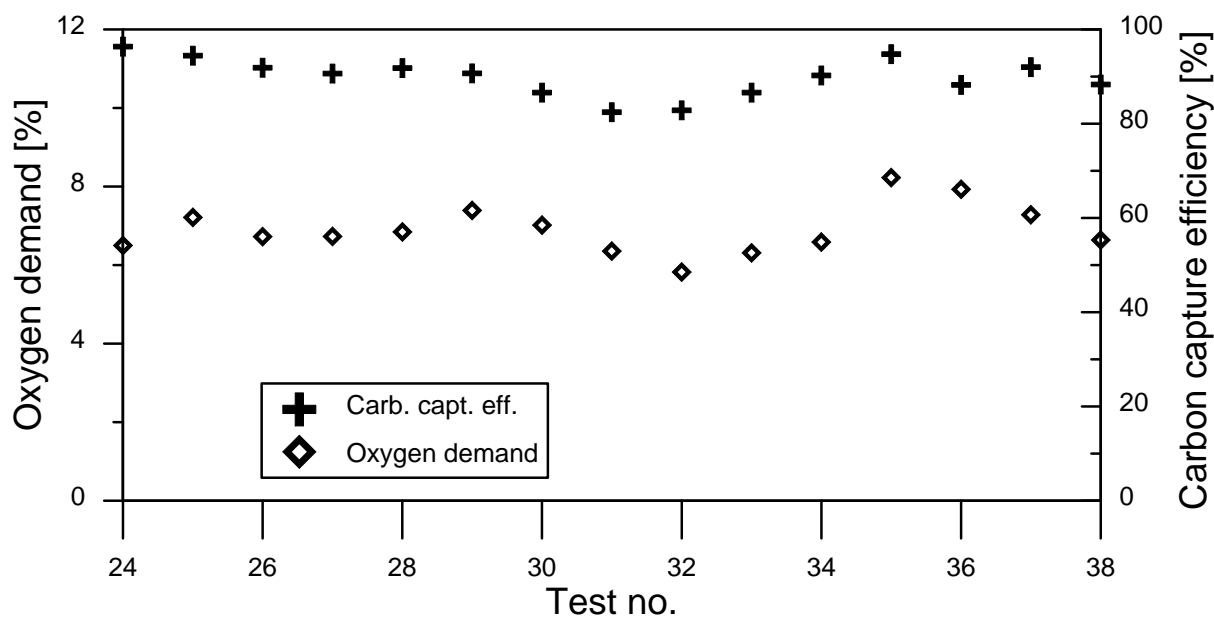
Fig. 16: Average values for oxygen demand and carbon capture for all Mangagran test periods.
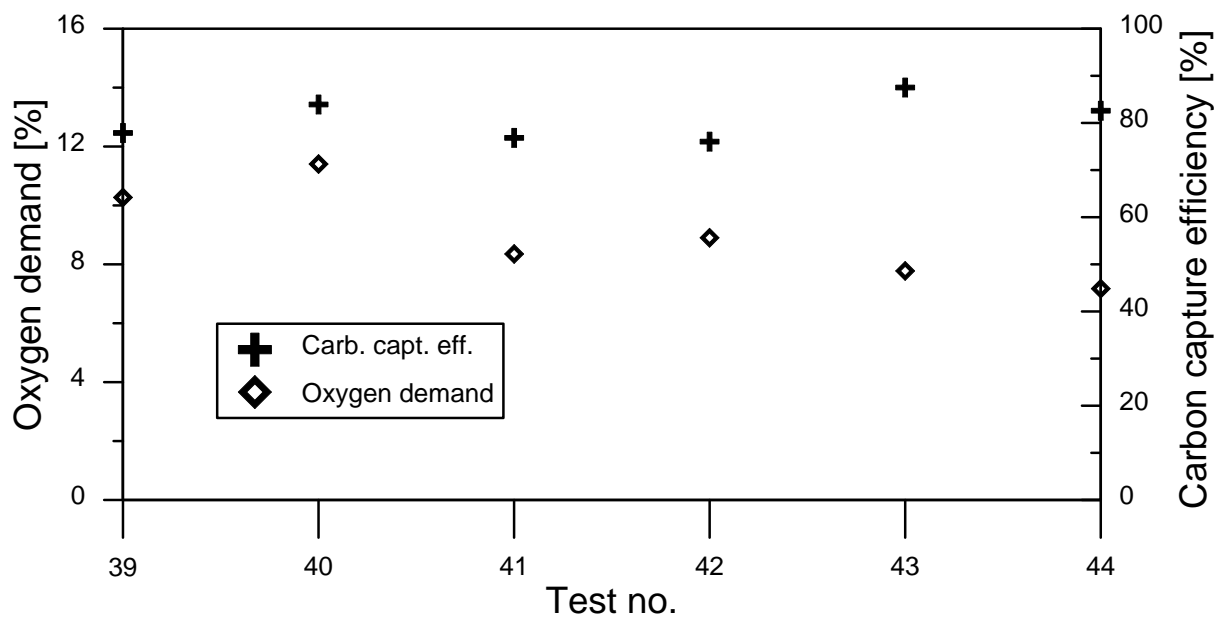
Fig. 17: Average values for oxygen demand and carbon capture for all Mesa experiments.

The Mesa tests had to be run at a lower temperature to avoid agglomeration, which had occurred in an earlier experiment with the same material. Poorer performance was therefore expected. When trying to increase the temperature over 925°C, the experiment had to be aborted due to agglomeration build-up. Upon opening of the reactor, it was found that the particles had formed both microagglomerates, s. Fig. 18, and a major macroagglomerate blocking about half the cross-section of the fuel reactor.

Fig. 18: Microagglomerates >500 µm formed after operation with Mesa.

The lifetime of the particles was calculated according to equations (14) and (15) based on fines production. While Mangagran and Mesa reached 109 and 99 h, respectively, Sinfin outperformed both with an estimated lifetime of 284 h. With Mangagran and Sinfin, no operational problems were encountered, although an increase in average particle size was observed for Mangagran.

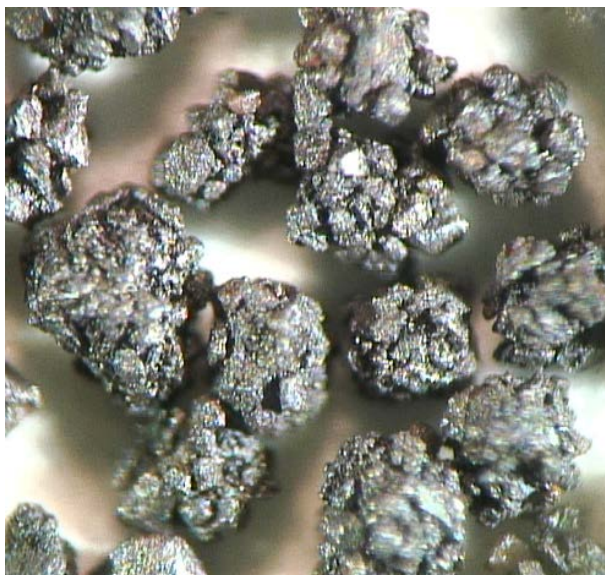For Sinfin, a few soft agglomerates were found when opening the reactor. Those fell apart when not handled carefully and are thus not seen as problematic.

3.4 Investigation of a Manufactured Material with High Sulphur Tolerance (Paper IV)

As mentioned in chapter 1 and found in the experiments conducted in paper II, materials containing calcium can be susceptible to sulphur poisoning. If an oxygen carrier such as calcium manganate is to be used mainly with low-sulphur biomass fuels, this disadvantage is considered an acceptable price to pay for the outstanding gas conversion performance found in paper I. However, a higher resistance of the material towards impurities found in fossil fuels would increase the robustness and flexibility of the process, allowing for concepts such as biomass co-firing.

In paper IV, a combined oxide of manganese and silicon with addition of titanium was operated for 32 hours and evaluated with respect to its performance and long-term stability. To obtain a robust database for potential future evaluations and to check the behaviour of the material when subjected to different fuel impurities, four different fuels (wood char, coal, pet coke and lignite) were tested. Also, these fuels cover a wide range of volatile contents – from 10% for pet coke to 45% for lignite – the influence of which was investigated as well.

Performance evaluation

Fig. 19 shows the oxygen demand for different fuels as a function of the circulation index at a fuel reactor temperature of 970°C.
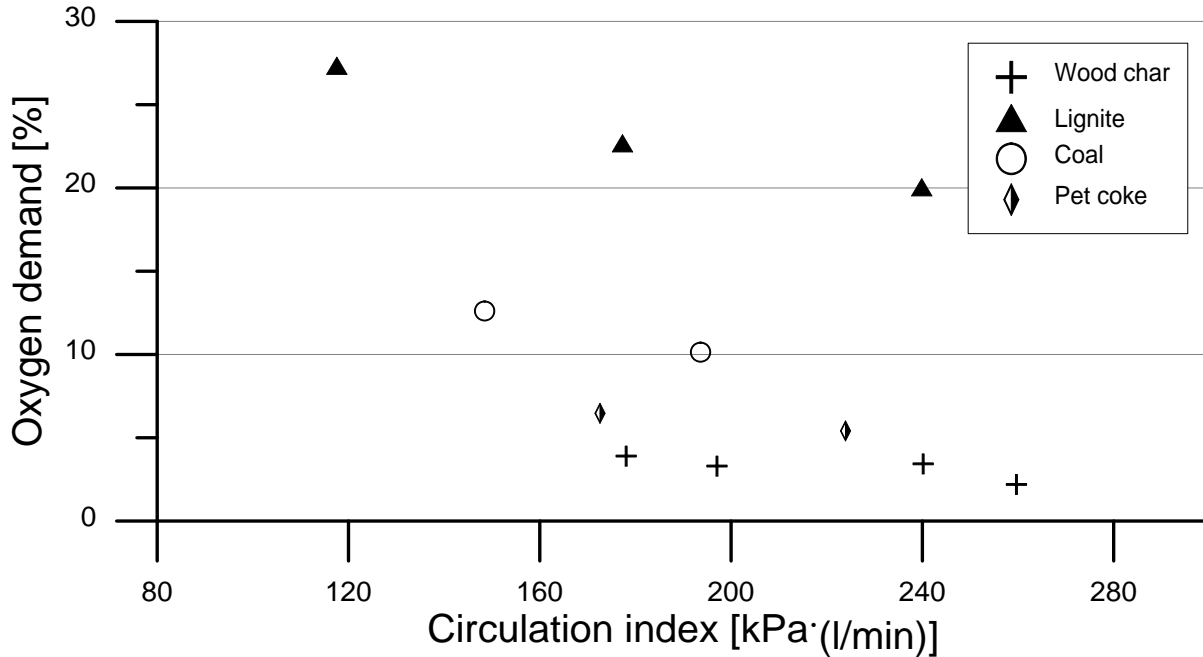

Fig. 19: Oxygen demand over circulation index, 970°C.

The trend towards better gas conversion at higher circulations is clear. Also, the fuel with the highest volatile content, lignite, performed worst in terms of gas conversion with a lowest average oxygen demand of 20%. The two low volatile fuels pet coke and wood char performed best, with wood char reaching an oxygen demand of 2.2% as mentioned earlier.

As opposed to its comparably low gas conversion, lignite reached very high carbon capture rates of 99.5%, which indicates a high reactivity of the char residue remaining after devolatilization. Pet coke had the lowest carbon capture efficiency, which is in line with previous findings that char stemming from pet coke is less reactive than biomass char because it has less active sites, is less porous and contains less catalytic elements [62]. However, the performance shown with pet coke (highest average carbon capture efficiency 90.2% at 970°C) is remarkable and the highest ever reached for this fuel in the 10 kW unit.

For all fuels but lignite a clear decrease of carbon capture efficiency at higher solids circulation could be seen. This correlation was expected due to the lower char residence time in the fuel reactor at high circulations, see Fig. 20.
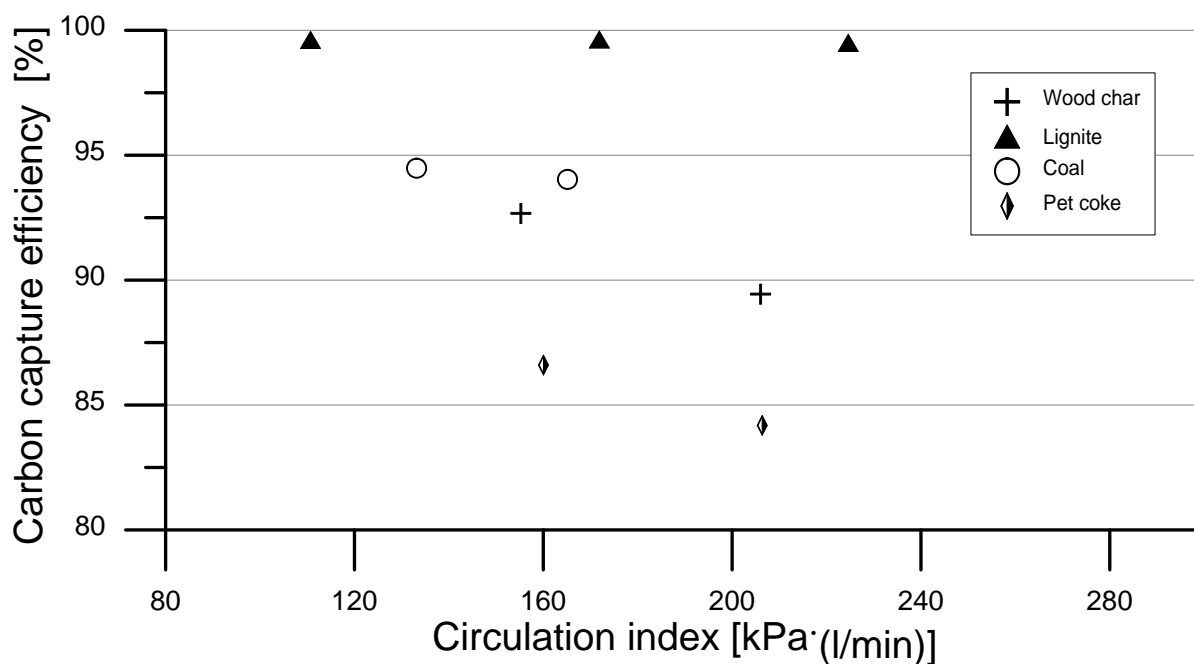
Fig. 20: Carbon capture efficiency over circulation index, 935°C.

Higher temperatures generally led to both better carbon capture efficiency and gas conversion. Fig. 21 and Fig. 22 show this relationship for all fuels and circulation rates.
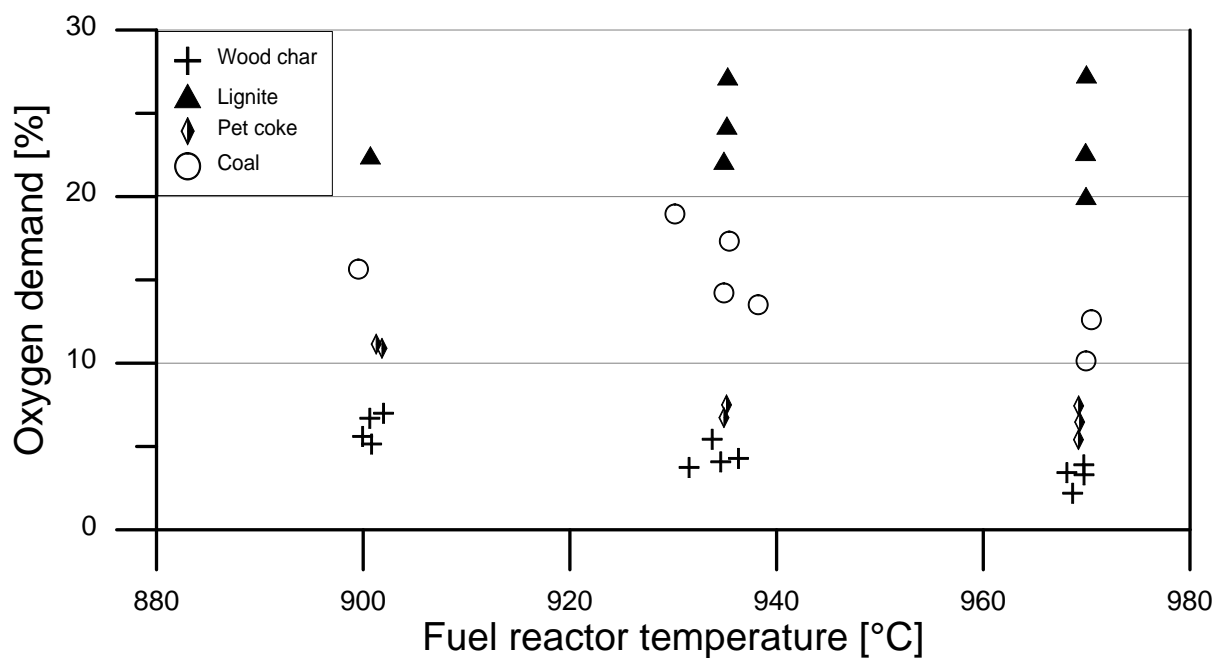
Fig. 21: Oxygen demand as a function of temperature.

For all fuels but lignite there is a strong trend towards higher carbon capture efficiency with increasing temperature. As no negative impacts of the elevated temperature level could be

31

detected, it can be concluded that this particular oxygen carrier is best suited for high temperatures.
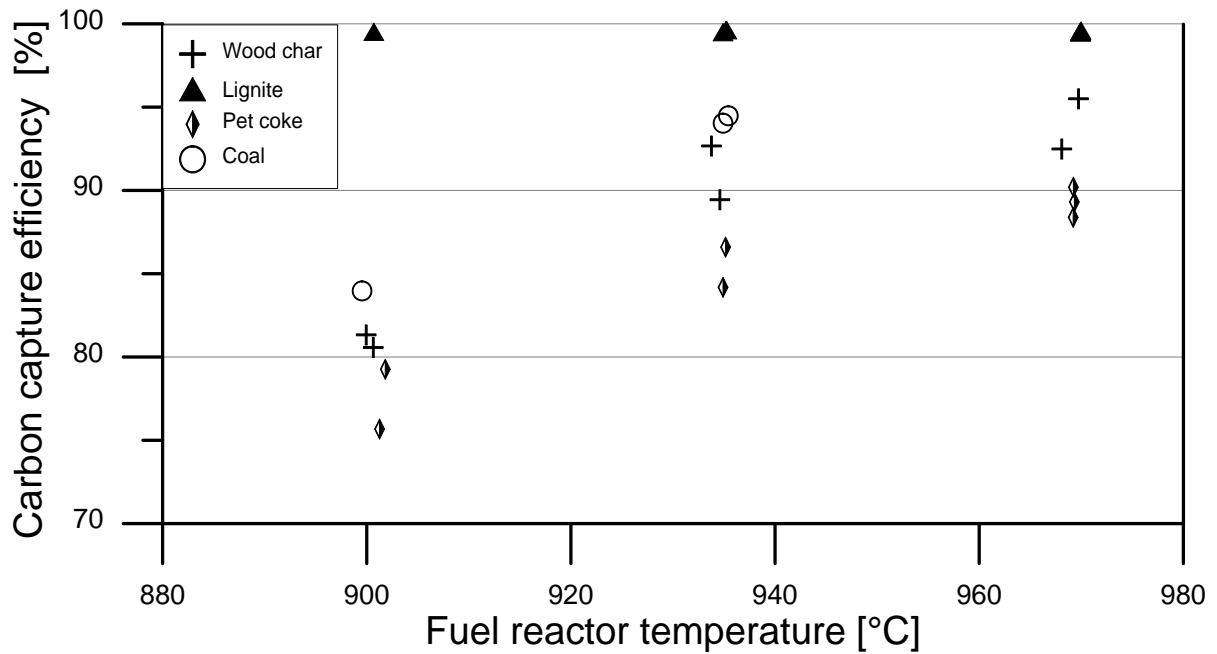
Fig. 22: Carbon capture efficiency as a function of temperature.

Particle mass balance and lifetime

As a consequence of mechanical and chemical stress in the process, the lifetime of the oxygen carrier material is limited. Here, the oxygen carrier particles are considered as spent as soon as they have become fines, in this study defined by a size below 63 μm.

Overall mass balance

A mass balance over the incombustible solids shows that some material was missing after the experiments were finalized, see Table 2.

Table 2: Mass balance of in- and outgoing incombustible material.

	IN	OUT
Incombustible solids [g]		
Oxygen carrier (including fines)	17000	17443
Ash	651	
Balance (=mass missing)	208	

As both fuel and oxygen carrier are handled manually during several steps of testing (filling and emptying the reactor system, reintroducing elutriated particles, sieving and weighing), some mass

loss is inevitable. Also, some material may escape through the filter bags downstream the air reactor. Other sources of uncertainty are the fuel ash analysis and the possibility of chemical changes, i.e. the oxidation state, in the oxygen carrier material. Altogether, these possible errors led to a missing mass of 208 g (or around 1.2%), which was assumed to be completely made up by fines, thus giving a more conservative estimate of the oxygen carrier lifetime, see Table 3.

Table 3: Mass balance of in- and outgoing incombustible fines.

	IN	OUT
Incombustible fines [g]		
Ash fines	456 (0-651)	-
Initial fines content	799	-
Fines in reactor upon opening	-	65
Fines elutriated from fuel reactor	-	525
Fines elutriated from air reactor	-	542
Mass missing from Table 2	-	208
Sum	1255	1340
Balance (=total oxygen carrier fines produced)	**85 (0-541)**	
Lifetime [h]	**5600 (880-∞)**	

Particles elutriated from the fuel reactor are a mixture of oxygen carrier, unconverted char and ash. While the char was removed by heating the sample to 900°C in air for 72 hours, the share and size distribution of the ash was determined using another approach: in a previous study, Linderholm et al. [69] found that when burning individual samples of coal and wood char in an oven at 900°C, around 70% of the resulting ash was fines. The same ratio was used for the current study. Knowing the total amount of ash fed with the fuel, this led to the assumption that 456 g of ash fines were present in the total mass of fines.

With that assumption, the total production of oxygen carrier fines becomes 85 g, corresponding to a lifetime of 5600 hours. Fig. 23 depicts all incombustible material flows with the ash fines shown in yellow, other ash material in green and oxygen carrier fines formed in the process in red.
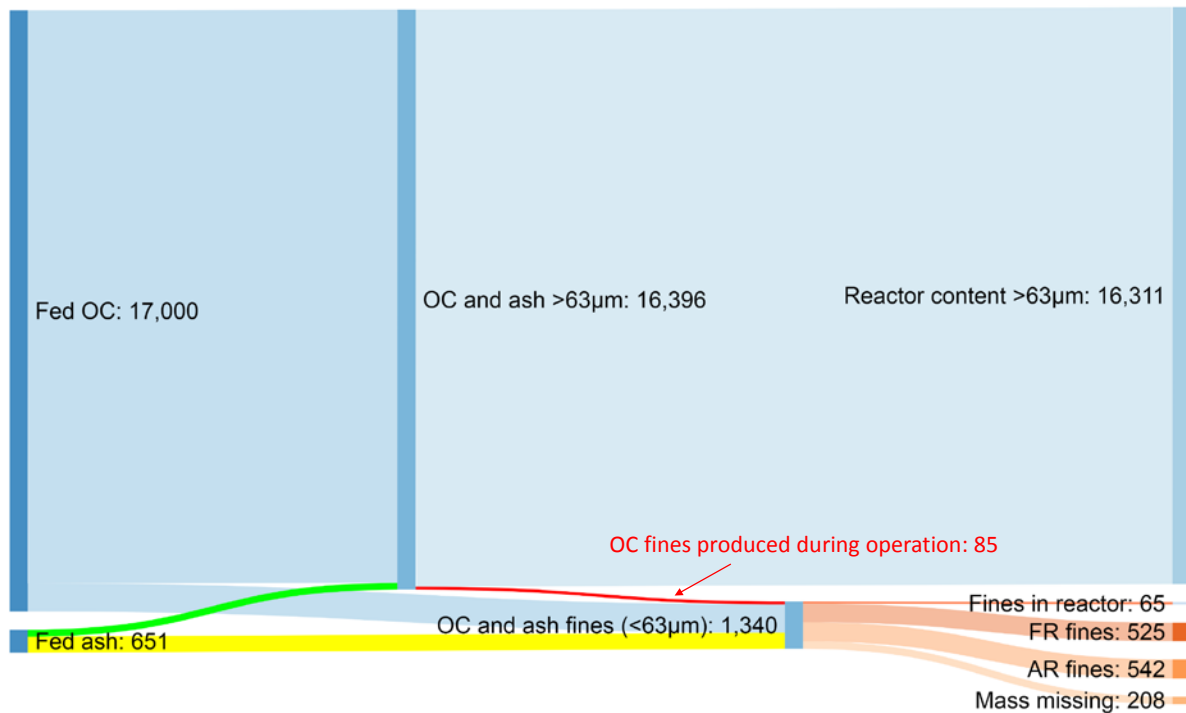
Fig. 23: Sankey diagram showing the fate of incombustible particles. All masses in g.

The diagram shows that the calculated mass of oxygen carrier fines produced depends on two critical assumptions, firstly the assumed fines content of the ash; secondly the assumption that the error in the mass balance is lost fines.

As for the first assumption, it could be argued that the ashes from burning coal in an oven do not give a realistic estimate of the harsh conditions present in a fluidized bed and that the ash content should be expected to turn to fines to a higher degree. Assuming that 83% of the ash turns to fines, instead of 70%, would mean that no oxygen carrier fines were produced at all and that the lifetime is unlimited. If, on the other hand, the extreme assumption is made that all ash remains in the bed as particles larger than 63 μm, the fines production increases to 541 g, meaning a decrease in lifetime to 882 hours.

The second assumption, that the error in the mass balance is lost fines, seems reasonable when considering that fines are lost more easily than larger particles during sieving. On the other hand it could just be an error in the total mass balance shown in Fig. 23. If so, the mass of incoming fines exceed the fines recovered, suggesting that no fines are formed, i.e. an infinite lifetime.

In total, the overall mass balance of the fines clearly indicates that the lifetime of the particles is long, most likely thousands of hours and in any case sufficient for continuous chemical looping combustion with solid fuels, where the bed material lifetime might be controlled by ash fouling rather than particle attrition.

3.5 Up-scaling to a 100kW Unit (Paper V)

Following the promising results that had been achieved with manganese ores in paper III, the aim of paper V was to upscale operation to the 100 kW reactor. The 10 kW unit was operated for 22 hours and the 100 kW unit for 34 hours with a sintered manganese ore and six different fuels. The 10 kW unit was mainly operated with Swedish and German wood char, the 100 kW unit with both wood char, black pellets and coal.

10 kW experiments

As an example of a typical experiment using different fuels, Fig. 24 shows the gas concentrations during a period of about 4 hours.
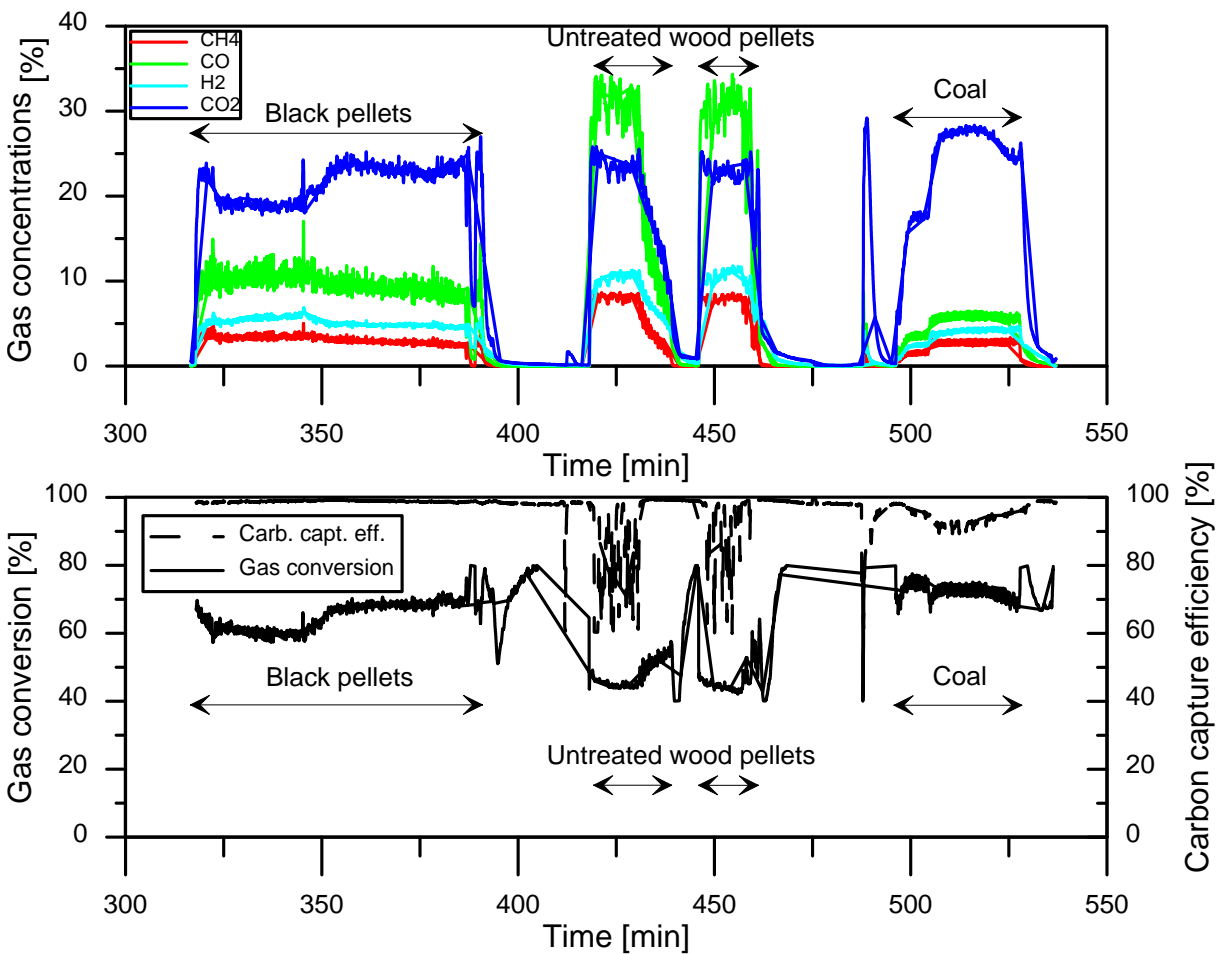
Fig. 24: Top: Gas concentrations in 10 kW experiments. Wood pellets testing done at very high fuel power. Bottom: Carbon capture and gas conversion for the same experiments.

As mentioned before, the choice of fuel greatly affects the conversion of combustible gases to CO_2 and water. In Fig. 24, the best performance is reached with coal, more unconverted species are present with the high-volatile black pellets. During testing with untreated wood pellets, the

concentration of CO even exceeds that of CO_2, placing the process closer to CLG (chemical looping gasification) rather than CLC.

At a fuel reactor temperature of about 970°C, gas conversion for black pellets was up to around 70%, for coal between 70 and 80% and for untreated wood pellets below 50%. This can be compared to the best value for wood char, around 93.5%. With respect to carbon capture, the picture is somewhat different; biomass char is known to be reactive because of its porous structure and catalytic properties of its ash components [62]. This is reflected in almost complete carbon capture (around 99%) for black pellets, while coal only reached 93%.

When analyzing the effect of the fuel used on the reactor's performance, two main factors could be identified as having an influence: volatiles content and particle size.
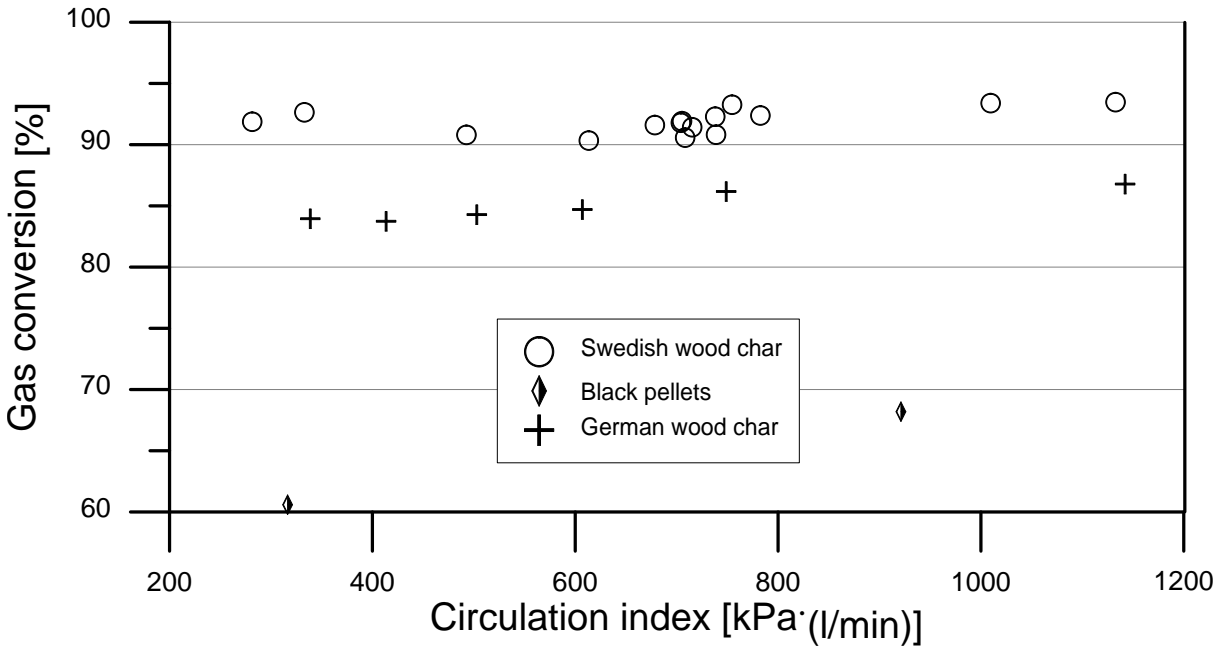
Fig. 25: Gas conversion in 10 kW experiments for different fuels. T_{FR}=970°C. Fuel power: Swedish wood char 3.3-5 kW, black pellets 4.1 kW, German wood char 5.4 kW

Fig. 25 shows gas conversion over circulation index for three different fuels. While a clear effect of higher solids circulation could not be established, the effect of the fuel type on gas conversion is evident. With ratings of 60-70%, the high-volatile black pellets perform considerably worse than the low-volatile wood chars. These, in turn, exhibit different behaviour despite their comparable chemical composition. The larger Swedish wood char particles show conversion rates above 90% at all tested circulation rates, while the smaller German wood char never reaches this value. When looking at carbon capture efficiency, see Fig. 26, this picture is reversed: almost full carbon capture (up to 98.4%) is reached with German wood char regardless of solids circulation, but with Swedish wood char the best value is 92.8%. Also, with this fuel a clear correlation with the

circulation index can be observed, with carbon capture decreasing as far as to 79.1%. The excellent gas conversion rates for the Swedish wood char shown in Fig. 25 thus come with the disadvantage of more char particles evading gasification and the choice of fuel size becomes a trade-off between gas conversion and carbon capture.
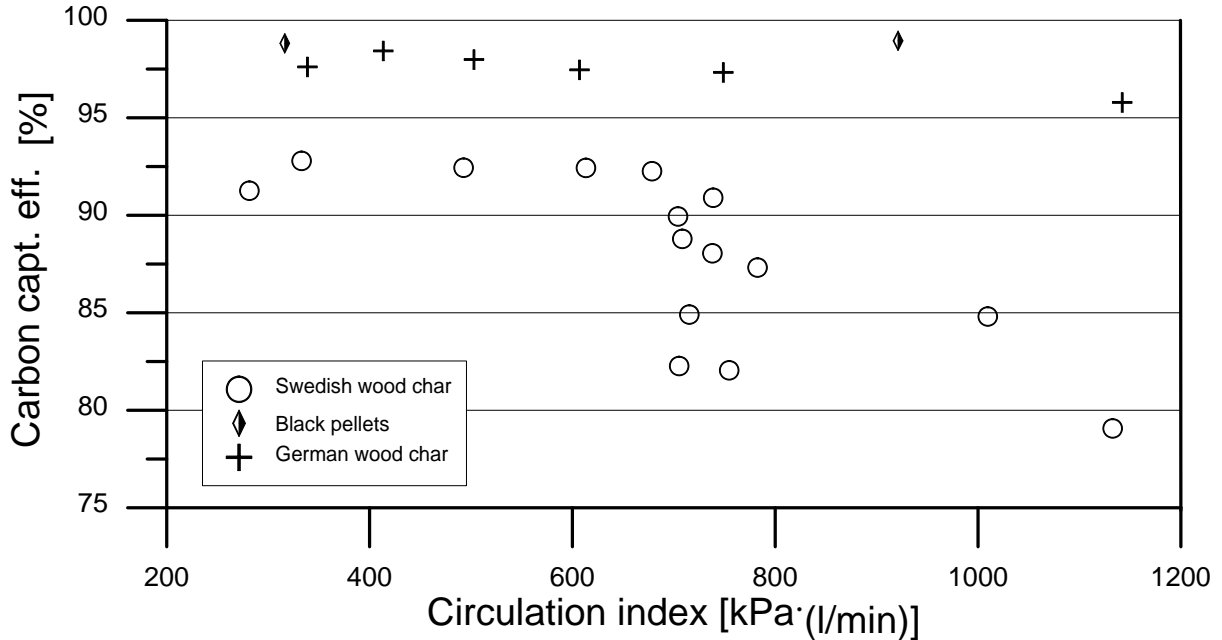
Fig. 26: Carbon capture efficiency in 10 kW experiments for different fuels.

The highest carbon capture of all fuels, around 99% and thus within the range of measurement errors relative to complete capture, is reached with black pellets. The likely explanation for that behaviour is, again, to be found in the different volatile contents. For wood char, a higher percentage of the heating value stems from char, which has to be gasified for conversion. With fixed carbon values of about 74% for wood char and less than 19% for black pellets, the amount of char to be gasified – or being able to slip to the air reactor before gasification can be completed – differs by a factor four at the same fuel power.

100 kW experiments

In the 100 kW unit, stable operation was reached with coal, crushed black pellets and two sizes of German wood char.

The specific bed inventory, expressed in kg oxygen carrier inventory in the fuel reactor per MW fuel power, has shown a correlation with gas conversion in previous experiments. For most of the test periods, the bed inventory was between 300 and 600 kg/MW, for larger wood char particles 800-900 kg/MW. In comparison, the 10 kW reactor used 1200-2100 kg/MW. Similar to that unit, a correlation between the fuel's volatile content and size, and gas conversion could be seen in

the 100 kW testing. The highest gas conversion of 93.5% was reached with the larger wood char particles. Also, higher gas conversion could be observed for increasing FR inventories, see Fig. 27.
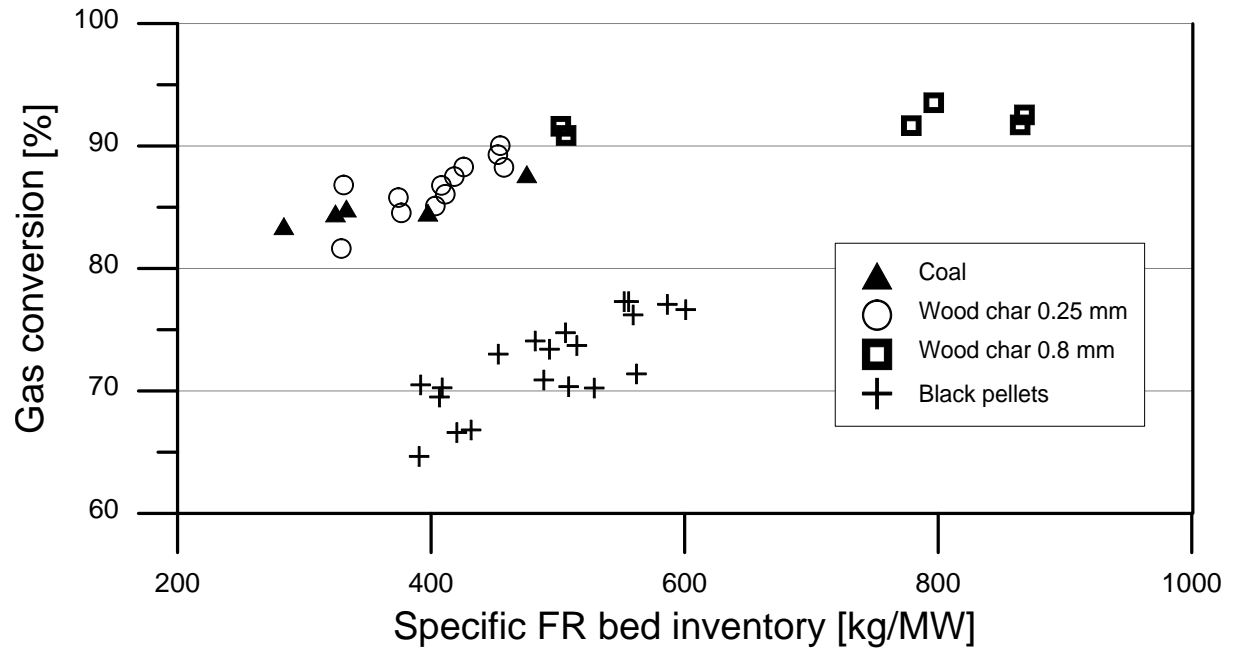
Fig. 27: Gas conversion over bed inventory for different fuels, 100 kW. T_{FR}=940-981°C

Several other manganese materials have previously been tested in the 100 kW unit, among which a mix of ilmenite and manganese ore and another sintered material. Fig. 28 shows a comparison of the tested manganese materials with ilmenite as base-line when using coal as fuel.
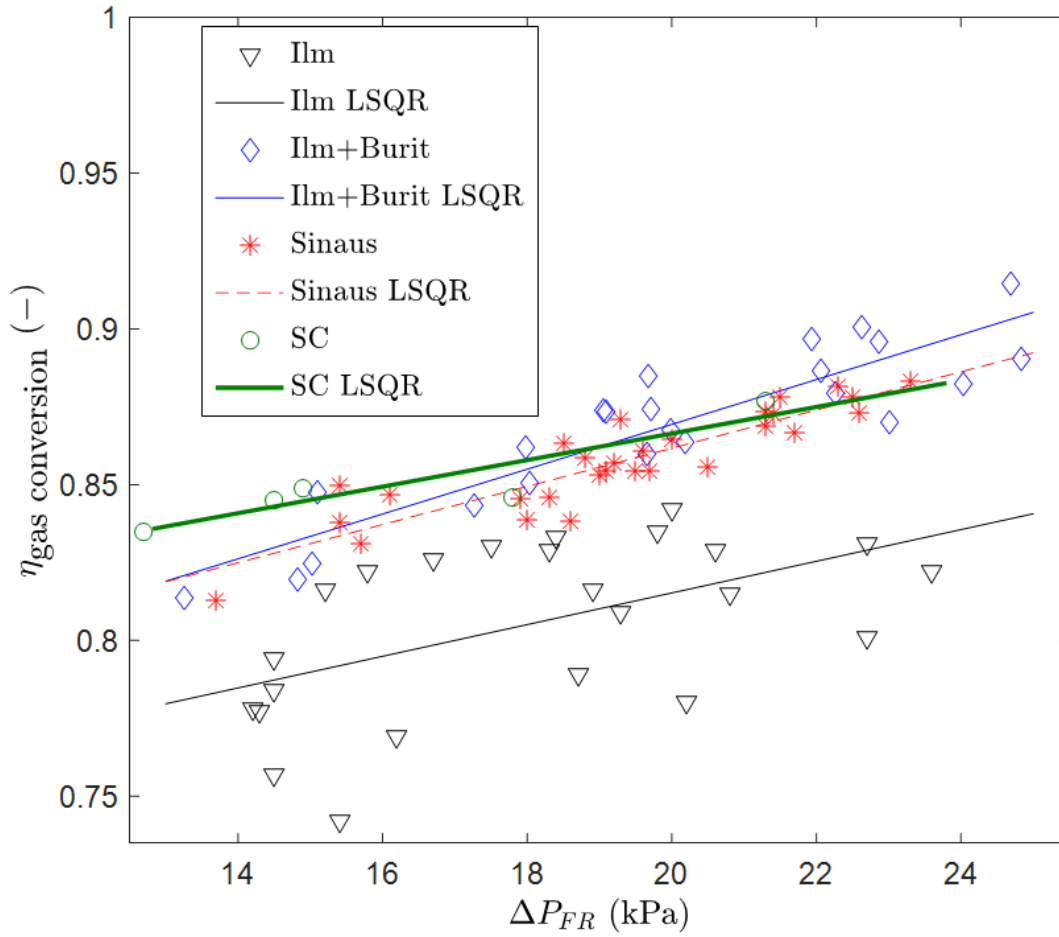
Fig. 28: Gas conversion efficiency over solids inventory in the fuel reactor showing combined operational experience with coal as fuel and as oxygen carrier: (i) ilmenite ("Ilm") [80], (ii) mixture of ilmenite and Buritirama manganese ore ("Ilm + Burit") [81], (iii) Sinaus [69], (iv) Sibelco Calcined, present results. LSQR: least-square regression (trend lines).

All manganese materials showed comparable gas conversion, which was distinctly superior to ilmenite. Carbon capture in the 100 kW was essentially complete for biomass fuels and between 97 and 99% for coal.

Particle mass balance and lifetime

As a means of forecasting the lifetime of the oxygen carrier material, global particle mass balances were established for both units. For the 100 kW unit, individual filter samples were used as input for lifetime calculations as well.

10 kW unit

Table 4 shows a summary of the accumulated in- and outgoing fines, which lead to a calculated lifetime of 745 hours.

Table 4: Mass balance of in- and outgoing incombustible fines.

	IN	OUT
Incombustible fines [g]		
Ash fines	458 (0-654)*	-
Initial fines content	162	-
Fines in reactor upon opening	-	73
Fines elutriated from fuel reactor	-	436
Fines elutriated from air reactor	-	487
Mass missing from global balance	-	125
Sum	620	1121
Balance (=total oxygen carrier fines produced)	**502 (306-960)***	
Lifetime [h]	**745 (390-1223)***	

*depending on amount of ash turning into fines

The lifetime depends on the fines share of ashes and lies between 390 (assuming no ashes turn into fines) and 1223 hours (assuming all ashes turn into fines).

100 kW: overall particle mass balance

As opposed to the 10 kW unit, the material flows in the 100 kW reactor do not allow for an analysis of all in- and outgoing flows during operation. Due to the layout of the system – the exhaust streams from fuel reactor and air reactor are merged before entering the wet scrubber – all particles elutriated from the system end up in wet filters and thus cannot be handled instantly. Instead, all filter material was air dried, weighed and homogenized in dry state before taking samples, which were treated analogously to the scheme described in paper IV. The results were then extrapolated from the samples to the bulk material.

Despite the size and complexity of the unit, an attempt was made to close the total mass balance over the whole test duration. Of 435 kg oxygen carrier material filled during the experiments, around 424 kg could be accounted for, a satisfactory result for a lab unit of this size. However, it should be noted that the level of confidence for the results is lower than in the 10 kW unit because handling, sieving and weighing inaccuracies are magnified by extrapolation from samples.

To obtain a complete picture of fines production in the unit, two different paths were chosen: a complete fines balance similar to the 10 kW unit, always bearing in mind the higher inaccuracies

coming with increasing reactor size, and an analysis of individual filters. The latter is made possible because both fuel reactor and air reactor particles end up in the filter after a short period during start-up when some particle accumulation takes place downstream the POC until steady state is reached. This is not the case in the 10 kW unit, where fuel reactor particles accumulate in the exhaust pipe and water seal and not in a filter. As a consequence, filters in the 100 kW reactor can be deliberately changed before and after parameter changes are made, enabling an analysis of the effect said changes have on the oxygen carrier.

100 kW: lifetime based on filter samples

Fig. 29 shows calculated lifetimes based on filters containing particles elutriated during stable operation with fuel in a chronological order.
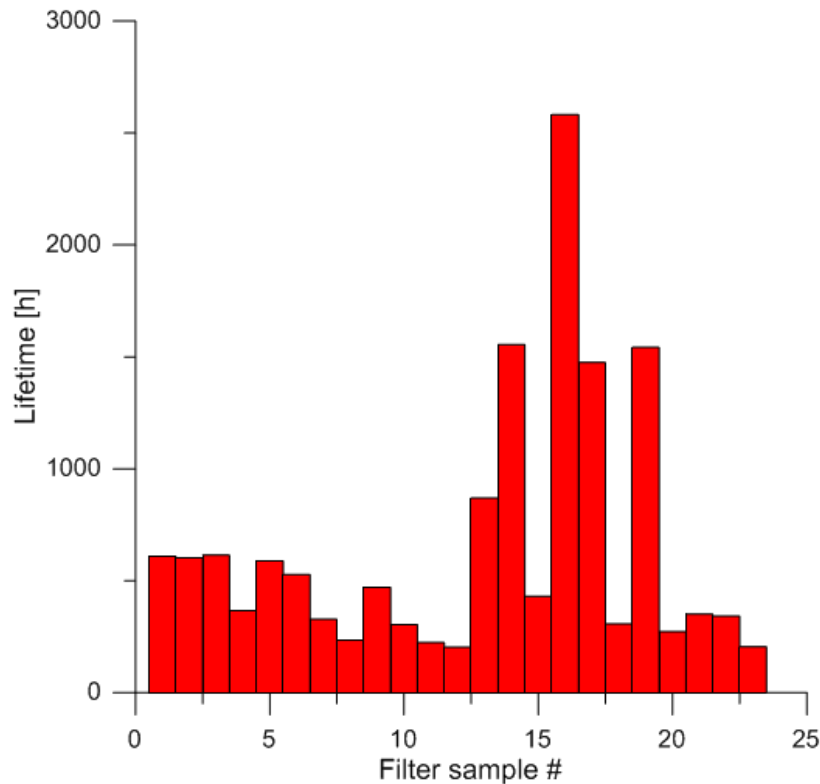
Fig. 29: Lifetime of the oxygen carrier based on filter samples from 100 kW unit.

The lowest lifetime based on filter samples was about 200 hours, with some samples showing results of several thousand hours. The time-weighted average over all shown filter samples was 707 hours. A clear trend over time is not evident, neither a correlation with fuel type.

Not all filter changes were made in synchronization with operational changes, meaning that some lifetime bars in Fig. 29 represent a mixture of different operating conditions. Fig. 30 shows the lifetime as a function of oxygen carrier conversion for those filter samples where parameter

changes were well synchronized with filter changes. Different intervals of solids circulation are marked in different colours. All samples represent an operational period with fuel feeding, dedicated hot operation tests without fuel were not done.
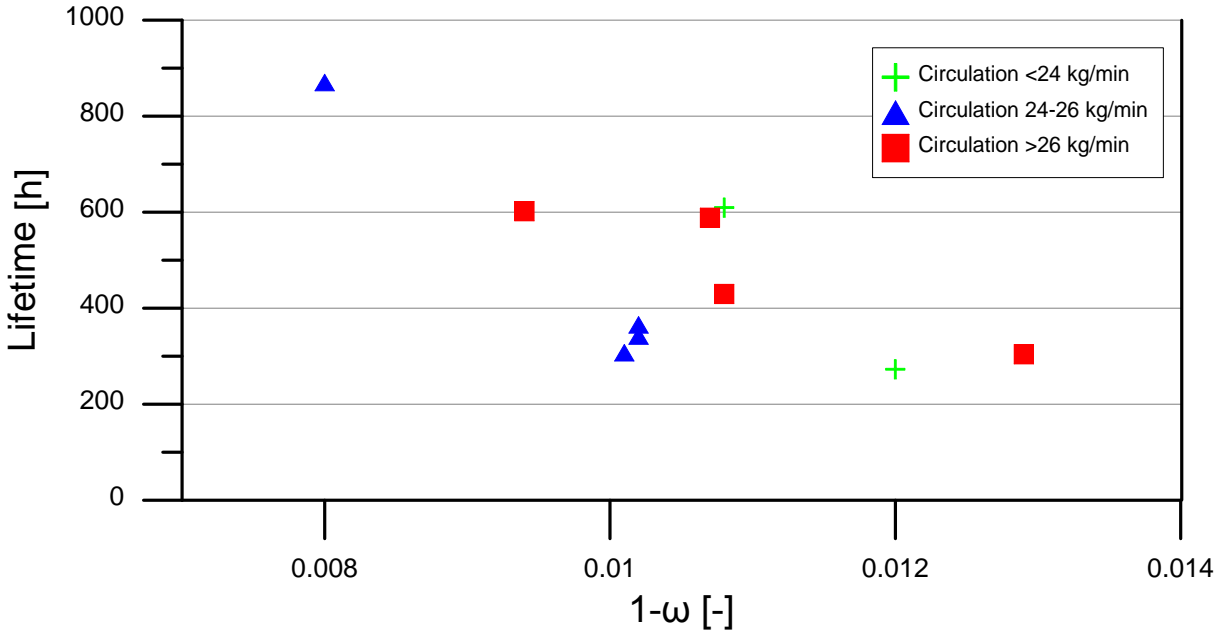
Fig. 30: Lifetime of the oxygen carrier as a function of oxygen carrier conversion.

A higher degree of oxygen carrier reduction clearly correlates with decreasing lifetime, showing the importance of chemical influences for particle durability. On the other hand, a direct influence of solids circulation on the lifetime was not seen. Thus, the data imply that mechanical wear played a smaller role than chemically induced stresses in the particle lifetime, at least in phases where fuel was present. However, it should be noted that mechanical attrition was nonetheless present, reflected by the fact that fines were found in the filters also in periods without fuel feeding.

100 kW: global fines balance

Following the second path to obtain a particle lifetime, samples of all known material streams, i.e., the material retrieved from the exhaust pipe downstream the POC, the remaining reactor content after experiments were finished and the content of *all* filters, regardless of operating conditions, were investigated as to their oxygen carrier fines content, adopting the methods and assumptions mentioned earlier. The resulting fines production over the whole test period was 32.7 kg, translating to a lifetime of 208 hours. This is considerably shorter than the average lifetime identified by filter sampling, the reasons of which are discussed in the next section.

Comparison of lifetime results in 10 and 100 kW units:

The comprehensive analysis of bed material led to a number of different lifetime readings reaching from around 200 hours as lowest lifetime acquired from individual filter samples over 745 hours as a result of a global fines balance in the 10 kW unit up to several thousand hours for other filter samples. The global fines balance in the 100 kW unit yielded a lifetime of 208 hours. The difference between the units can be explained by two factors:

Firstly, the actual number of fuel hours was used in the lifetime calculation, not the total fluidization duration in the system. Due to its size and complexity, the 100 kW unit needs more time for heating and cooling, leading to higher hot fluidization durations than in the 10 kW unit. As the particles also break down with no fuel present, a shorter lifetime was expected.

Secondly, the fuel reactor in the 100 kW unit is designed as a circulating fluidized bed, as opposed to the bubbling fluidized bed in the 10 kW unit, which entails higher fluidization velocities and might make a difference in mechanical wear of the particles.

Anyhow, assuming an average lifetime in the range of 200-750 hours, the tested oxygen carrier is the most durable natural manganese material tested in both the 10 and 100 kW reactors to date. Table 5 shows the lifetime of all materials in this category which were successfully investigated in these units and, in comparison, the lifetimes of ilmenite and an iron ore.

Table 5: Lifetimes of natural manganese oxygen carriers and two reference materials.

Oxygen carrier	Reactor	Lifetime [hours]	Reference**
Sibelco Calcined	10 kW, 100 kW	200-750*	Paper V
Sinfin	10 kW	284	Paper III
Mangagran	10 kW	109	
Mesa	10 kW	99	
Buritirama	10 kW	48	[58]
Sinaus	100 kW	100-400	[69]
Tierga iron ore	100 kW	280-375	[39]
Ilmenite	100 kW	700-800	[70]

*Some filter samples suggested lifetimes of several thousand hours. The highest values are discarded here.

**In all the cited studies, a smaller particles size was used as definition of fines (45 instead of 63 µm), which means that the results presented here give a more conservative estimation of the particle lifetime.

3.6 Uncertainties

As is usually the case in experimental research, the data collected in this study is prone to a series of errors, which can affect the validity of the results found. These errors can be roughly divided into 3 categories:

1. Instrument-related errors:

Getting a reliable reading on the data fed into the calculation of the performance indicators defined in section 2.5 is crucial for the credible assessment of system performance. Gas flows, temperatures, pressure drops and gas concentrations are measured online and thus subject to measurement errors.

Apart from online measurements, the flows of fuel (both units) and steam (10 kW unit) were only recorded as average values by weighing the water- and fuel tanks before and after operation. Because the focus was on continuous operation rather than on the examination of transient behaviour, this solution should be acceptable in the study's context.

It should be noted that no higher hydrocarbons and tars were measured in the experiments. Although this might be acceptable when using fossil fuels, biomass is expected to form more tars which consequently should be accounted for in the mass balance.

2. Sampling errors:

Especially in the 100 kW unit, where not all material can be heat-treated and sieved, a potential error is introduced by material sampling and handling. Taking a representative sample from a bucket of material is not trivial and deviations in fines- and char content can be substantial. To understand and control this influence, the material batches were homogenized before sampling and for batches containing a lot of material, several samples were taken from different spots.

Another uncertainty is introduced by the chemical analyses of fuel and oxygen carrier which were performed at an external lab.

3. Handling, operational and equipment-related errors:

When handling large amounts of oxygen carrier and solid fuel in a lab environment, some loss of material is inevitable despite the best efforts to avoid this, see section 3.4. Nevertheless, the nature and size distribution of the missing material is unknown, which is why assumptions have to be introduced. Concerning the lifetime analyses, incomplete sieving might have some impact on the end result. In papers IV and V, the samples were dry-sieved as opposed to wet sieving in paper I-III, making the direct reintroduction of particles > 63 μm elutriated from the air reactor possible. To check whether the same degree of separation could be achieved with dry sieving as

with wet-sieving, some samples were divided and treated with both methods, showing a negligible difference.

Another factor which might influence the mass balance is insufficient emptying and cleaning of the reactor, the impact of which was tried to minimize by sophisticated cleaning equipment and camera inspection of the reactors after emptying. Also, leakage of gases on their way into or out of the reactor might occur, which is why regular high pressure leak tests were performed. Table 6 summarizes the known measurement errors mentioned above.

Table 6: Measurement errors. Percentages relative to measurement value unless marked otherwise.

Instrument/variable	Measurement error
Mass flow control	<1% of measurement range
Temperature	2°C
Gas concentrations	1%
Pressure transducers	0.5%
Chemical analyses	0.1-0.5%
Calibration gases	0.2-0.5%
Scales	0.1-0.5 g

Due to the high reliability of the most important measurements, i.e. gas concentrations for conversion performance assessment and masses for lifetime calculations, the impact of the mentioned errors is, although hard to quantify, believed to be small.

4. Discussion

Table 7 compares the performance indicators of all tested materials in the 10 kW unit with two reference materials. The main differences between the tested manganese ores lie in their mechanical properties and durability rather than in their performance. As not all materials were tested with all fuels, the selection is limited to experiments with wood char and pet coke.

Table 7. Performance comparison of all tested materials in the 10 kW unit with two reference materials (average values)*. Only tests with wood char and pet coke shown.

	Calcium manganate (paper I,II)	Mangagran (paper III)	Sinfin (paper III)	Mesa (paper III)	Mn-Si-Ti (paper IV)	Sibelco Calcined (paper V)	Ilmenite [58]	Buritirama [79]
Gas conversion (wood char/ pet coke) [%]	96.5	93.0	92.8	92.6	95.8	91.9	-	-
	91.4	-	87.6	-	93.0	-	80	85
Carbon capture (wood char/ pet coke) [%]	92.6	90.5	93.1	84.7	93.0	88.3	-	-
	88.2	-	72.5	-	88.0	-	66	94
Fuel power (wood char/pet coke) [kW]	3.9	3.6	4.9	3.9	2.6	3.8	-	-
	7.1	-	17.2	-	3.9	.	5.9	5.9
Lifetime [h]	-**	109	284	99	5600	745	-**	48
Temperature [°C]	970	970	970	925	970	970	970	960

*The depicted gas conversion and carbon capture values represent a time-weighted average over all experimental periods made at the same temperature (apart from Mesa, which could not be operated at that temperature, see Paper III) and thus do not reflect the best achieved values.

**Lifetime not calculated in 10 kW solid fuel unit

Spray-dried particles:

Of the materials tested in this study, calcium manganate offers the highest average gas conversion with wood char as fuel, which is assumed to be a result of the CLOU effect. Also, the highest individual gas conversion value was reached with this material, although Mn-Si-Ti came close (97.9 and 97.8%, respectively). For low circulation rates, calcium manganate reached up to 98.2% carbon capture. Increasing the temperature to 1030°C boosted this number even further

to 98.7%. Mn-Si-Ti was not tested at higher temperatures than 970°C. The highest carbon capture with the same fuel was 95.5% and reaching up to 99.6% using the highly-reactive – and volatile-rich – lignite. Neither calcium manganate nor Mn-Si-Ti showed signs of premature break-down and attrition, although a rigorous mass balance was only made for the latter. The lifetime retrieved from this mass balance suggests a lifetime an order of magnitude above the tested natural materials.

Natural materials:

In paper III, when using biochar and ores, the lowest oxygen demand was achieved for operation with Mangagran, the highest carbon capture with Sinfin. With pet coke, the performance of Sinfin was clearly better than that of ilmenite. With ilmenite as oxygen carrier using the same fuel in the same 10 kW unit, an oxygen demand of 20% and a carbon capture efficiency of 66% were reached [58]. As Sinfin performs better than ilmenite when using pet coke and shows similar performance as Mesa and Mangagran when using biochar, it can be concluded that all tested manganese materials are significantly more reactive than ilmenite, with calcium manganate and Mn-Si-Ti outperforming the manganese ores. Another manganese ore ("Buritirama") also performed better than ilmenite with 15% oxygen demand and 94% carbon capture in a previous study [79], although at the price of lower lifetime, which was estimated to 48 h based on fines production. The high value for carbon capture efficiency can in part be explained by the high potassium and sodium contents in Buritirama, which are known to catalyse gasification reactions [82]. Other reasons are the lower fuel power and solids circulation as compared to the current study.

The sintered material investigated in paper V, Sibelco Calcined, was slightly less reactive than Sinfin when tested with wood char but exceeded its lifetime almost threefold. Different fuels were tested with Sibelco Calcined, showing a connection between gas conversion, carbon capture efficiency and volatile content. Extrapolating the results reached with natural ores in paper III to these fuels would be speculative, but given a certain comparability in chemical composition and performance with wood char, the same promising outcomes would be expected.

Comparison of spray-dried and natural materials:

When burning biochar, oxygen demand could be more than halved as compared to the most promising material from paper III, Sinfin, by using the manufactured calcium manganate. In an industrial size unit, this would mean considerable savings in the oxygen polishing step. For pet coke, the same trend can be observed. All tested materials performed better compared to the reference materials ilmenite and Buritirama as far as gas conversion was concerned.

The raw materials for calcium manganate and Mn-Si-Ti are potentially cheap but the additional cost related to spray-drying is hard to estimate. Previous publications assumed 1 €/kg of oxygen carrier for spray-drying, calcination and sieving [83].

Performance comparison of 10 and 100 kW units:

Up-scaling operation from the 10 to the 100 kW unit showed that comparable or better gas conversion was possible with considerably lower specific fuel reactor bed inventory. The more sophisticated design of fuel reactor and carbon stripper in the bigger unit also reduced carbon slip to the air reactor.

Lifetime:

The lifetime of the oxygen carrier would be decisive for the use in an industrial size unit and has been found to be an issue for manganese ores in a previous study [79]. Ilmenite has previously been investigated in the 100 kW unit and its lifetime was found to be around 700 hours based on fines production [47], which is in the same range as for the most durable natural manganese material, Sibelco Calcined. However, the actual lifetime might be determined by ash removal and fouling of the oxygen carrier by the ash rather than oxygen carrier attrition. Because of that, Lyngfelt and Leckner [71] conservatively estimate the lifetimes of manganese materials to 100 hours and for ilmenite to 200 hours for a 1000 MW chemical looping plant. At utility scale, the cost for oxygen polishing and potential longer lifetime would then have to be weighed against the additional cost of a manufactured oxygen carrier.

Concerning the cost of manganese ores as compared to ilmenite, Lyngfelt and Leckner assumed an ilmenite price of 175 €/ton and a manganese ore price of 225 €/ton, leading to a cost of 2 and 5 €/ton captured CO_2. This can be compared to an approximate CO_2 compression cost of 10 €/ton CO_2. Assuming a similar lifetime of for instance 100 h for both materials would reduce the difference in cost from 3 to 1 €/ton CO_2, while the total oxygen carrier cost would obviously decrease with longer lifetime.

In a utility-scale unit, a reduction in oxygen demand by 5%-units would save around 2.5 €/ton CO_2. Thus, it is clear that manganese ores have a potential for reducing costs, provided that their price does not differ too much from ilmenite. An option might be to mix these materials, as previously done by Linderholm et al. [41], who showed that the oxygen demand could almost be halved using a mixture of ilmenite and manganese ore.

5. Conclusions

The development of oxygen carrier materials with satisfying conversion properties and resilience towards the demanding conditions in reactive fluidized beds is an important factor in the upscaling of solid fuel chemical looping combustion. The ability of the material to be used efficiently with different kinds of fuels, both fossil and biogenic, while showing sufficient lifetime and being insensitive to sulphur poisoning and ash interaction is one key to economic viability of the process.

Although manganese materials have been known to possess characteristics relevant for chemical looping combustion, experimental experience with solid fuels and manganese materials was limited prior to this work. While it was known that higher gas conversion and carbon capture than with the state-of-the-art oxygen carrier ilmenite were possible, the lifetime issues related to manganese materials had not been addressed sufficiently.

In this study, six different oxygen carriers have been tested with respect to their reactivity and long-term integrity in 10 kW and 100 kW chemical looping combustors. The main findings are:

On the performance of manganese materials in general:

- The calcium manganate material $CaMn_{0.9}Mg_{0.1}O_{3-\delta}$ (papers I and II) performed better than ilmenite with respect to gas conversion and carbon capture efficiency. When used with sulphurous fuels, the oxygen carrier accumulated sulphur, which eventually might lead to worse performance. However, regeneration of the material by using low-sulphur fuel and a high fuel reactor temperature was possible. It can be concluded that $CaMn_{0.9}Mg_{0.1}O_{3-\delta}$ is suitable for chemical looping combustion of low-sulphur fuels, where it offers the potential of considerable cost reductions in utility scale. The suitability for use with sulphurous fuels likely depends on sulphur content and whether regeneration cycles would be possible during operation.

- The Mn-Si-Ti material tested in paper IV showed comparable performance. As this oxygen carrier is not susceptible to sulphur poisoning, it should be suited for flexible operation with both biomass and fossil fuels.

- The comprehensive fines mass balance established in paper IV showed that very high lifetimes can be reached for manufactured particles. Ash accumulation did not impair the performance of the material in the time-scale considered, but would have to be dealt with in longer operations.

- In paper III, two out of three manganese ores performed well in the process while one material formed agglomerations. All materials had higher gas conversion and carbon capture efficiency than ilmenite. The most durable material ("Sinfin") reached a lifetime of 284 hours based on fines production, which is almost six times longer than a previously tested manganese ore. In paper V, a sintered manganese ore reached a lifetime of 745 hours in the 10 kW reactor, placing the material in the same range as ilmenite as far as durability is concerned. In the 100 kW unit, the material reached lifetimes between 200 and 750 hours, depending on operating conditions. These findings indicate that manganese ores can combine high gas conversion with reasonable lifetime.

- A general conclusion is that manganese materials add to the flexibility and economic viability of the process. Further, they have shown to be durable in long-term operation and are therefore considered to be mature for the use in utility-size chemical looping plants.

Comparison of results from the 10 kW and the 100 kW unit:

- In both the 10 and 100 kW unit, essentially complete carbon capture can be reached for reactive fuels. Gas conversion performance was in part correlated with the volatile content of the fuel. If the conversion of the volatiles could be improved, the need for oxygen in the subsequent oxy-polishing step might be reduced or even eliminated.
- The 100 kW unit reached slightly higher gas conversion with roughly a third of the specific bed inventory as compared to the 10 kW unit.
- Lifetime calculations yielded different results for both units and are hard to compare due to the differences in operating conditions. Based on a global fines balance, the lifetime of the oxygen carrier was 745 and 208 hours for the 10 and 100 kW units, respectively. This result was based on longer hot fluidization, higher gas velocities and lower specific fuel reactor bed inventories in the 100 kW unit. All in all, Sibelco Calcined reached the highest lifetime recorded so far with natural manganese materials in these reactors, which is deemed to be more than sufficient for the process.

On the comparison between natural ores and manufactured materials:

- Comparing the manufactured oxygen carriers to the best-performing manganese ores, the oxygen demand was halved when using biochar. Whether a more expensive manufactured material or a naturally occurring manganese ore would be used in large scale will be a trade-off between oxygen carrier cost, the lifetime of the material and the cost of oxygen polishing.

On process variables:

- The size and volatiles content of the fuel clearly affect performance: for small particles and high volatile contents, carbon capture is almost complete at the expense of lower gas conversion. In scaling up, finding the optimal fuel size and designing an efficient volatile distribution system should be focal points of optimization.
- Gas conversion generally increased with higher bed inventory in the fuel reactor of the 100 kW unit.
- Higher circulation had a positive impact on gas conversion – in the 100 kW reactor only for certain fuels – at the expense of decreasing carbon capture efficiency.

References

[1] IPCC. Climate Change 2013: The Physical Science Basis Working Group I Contribution to the Fifth Assessment Report of the Intergovernmental Panel on Climate Change. In: Stocker T QD, Plattner G, Tignor M, Allen S, Boschung J et al, editor. Cambridge, United Kingdom and New York, NY, USA: Cambridge University Press; 2013.

[2] IPCC. Climate Change 2014: Synthesis Report. Contribution of Working Groups I, II and III to the Fifth Assessment Report of the Intergovernmental Panel on Climate Change. In: R.K. Pachauri LAM, editor. Geneva, Switzerland: IPCC; 2014.

[3] Luthi D, Le Floch M, Bereiter B, Blunier T, Barnola J-M, Siegenthaler U, et al. High-resolution carbon dioxide concentration record 650,000-800,000 years before present. Nature. 2008;453:379-82.

[4] Schmidt G, Ruedy R, Persin A, ., Sato M, K. L. ASA GISS Surface Temperature (GISTEMP) Analysis. In: Carbon Dioxide Information Analysis Center ORNL, U.S. Department of Energy, editor. Trends: A Compendium of Data on Global Change. Oak Ridge, Tenn., U.S.A.2016.

[5] Etheridge DM, L.P. Steele LP, Langenfelds RL, Francey RJ. Historical CO2 record derived from a spline fit (20 year cutoff) of the Law Dome DE08 and DE08-2 ice cores. In: Division of Atmospheric Research C, editor. Aspendale, Victoria, Australia 1998.

[6] Tans P, Keeling R. Trends in Atmospheric Carbon Dioxide. In: NOAA/ESRL, Oceanography SIo, editors.2018.

[7] John C, Dana N, Sarah AG, Mark R, Bärbel W, Rob P, et al. Quantifying the consensus on anthropogenic global warming in the scientific literature. Environmental Research Letters. 2013;8:024024.

[8] Arrhenius S. On the Influence of Carbonic Acid in the Air upon the Temperature of the Ground. Philosophical Magazine and Journal of Science. 1896;41:239-76.

[9] NOAA. State of the Climate: Global Analysis for Annual 2017. National Oceanic and Atmospheric Administration (NOAA), National Centers for Environmental Information; 2018.

[10] Kokic P, Crimp S, Howden M. A probabilistic analysis of human influence on recent record global mean temperature changes. Climate Risk Management. 2014;3:1-12.

[11] NOAA. State of the Climate: Global Analysis for Annual 2015. National Oceanic and Atmospheric Administration (NOAA), National Centers for Environmental Information; 2016.

[12] Donat MG, Lowry AL, Alexander LV, O'Gorman PA, Maher N. More extreme precipitation in the world's dry and wet regions. Nature Climate Change. 2016;6:508.

[13] Fetterer F, Knowles K, Meier W, Savoie M, Windnagel AK. Sea Ice Index, Version 3, updated daily. In: Center NNSaID, editor. Boulder, Colorado USA 2017.

[14] Diffenbaugh NS, Field CB. Changes in Ecologically Critical Terrestrial Climate Conditions. Science. 2013;341:486-92.

[15] UNFCCC. FCCC/CP/2015/L.9/Rev.1. Paris 2015.

[16] Anderson K, Bows A. Beyond 'dangerous' climate change: emission scenarios for a new world. Philosophical Transactions of the Royal Society A: Mathematical, Physical and Engineering Sciences. 2011;369:20-44.

[17] IPCC. Climate Change 2014: Mitigation of Climate Change. Contribution of Working Group III to the Fifth Assessment Report of the Intergovernmental Panel on Climate Change. In: Edenhofer O P-MR, Sokona Y, Farahani E, Kadner S, Seyboth K, et al, editor. Cambridge, United Kingdom and New York, NY, USA: Cambridge University Press; 2014.

[18] IEA. World Energy Outlook 2017. Paris: International Energy Agency; 2017.

[19] Lewis W, Gilliland E, Sweeney M. Gasification of carbon Chemical Engineering Progress. 1951;47:251-6.

[20] Lyon RK, Cole JA. Unmixed combustion: an alternative to fire. Combustion and Flame. 2000;121:249-61.

[21] Cao Y, Casenas B, Pan WP. Investigation of chemical looping combustion by solid fuels. 2. Redox reaction kinetics and product characterization with coal, biomass, and solid waste as solid fuels and CuO as an oxygen carrier. Energy and Fuels. 2006;20:1845-54.

[22] Scott SA, Dennis JS, Hayhurst AN, Brown T. In situ gasification of a solid fuel and CO2 separation using chemical looping. Aiche J. 2006;52:3325-8.

[23] Leion H, Jerndal E, Steenari BM, Hermansson S, Israelsson M, Jansson E, et al. Solid fuels in chemical-looping combustion using oxide scale and unprocessed iron ore as oxygen carriers. Fuel. 2009;88:1945-54.

[24] Leion H, Mattisson T, Lyngfelt A. The use of petroleum coke as fuel in chemical-looping combustion. Fuel. 2007;86:1947-58.

[25] Leion H, Mattisson T, Lyngfelt A. Solid fuels in chemical-looping combustion. International Journal of Greenhouse Gas Control. 2008;2:180-93.

[26] Lyngfelt A. Chemical-looping combustion of solid fuels - Status of development. Appl Energ. 2014;113:1869-73.

[27] Mattisson T, Lyngfelt A, Leion H. Chemical-looping with oxygen uncoupling for combustion of solid fuels. International Journal of Greenhouse Gas Control. 2009;3:11-9.

[28] Jerndal E, Mattisson T, Lyngfelt A. Thermal Analysis of Chemical-Looping Combustion. Chemical Engineering Research and Design. 2006;84:795-806.

[29] Berguerand N, Lyngfelt A. Chemical-looping combustion of petroleum coke using ilmenite in a 10 kW$_{th}$ unit-high-temperature operation. Energy and Fuels. 2009;23:5257-68.

[30] Cuadrat A, Abad A, García-Labiano F, Gayán P, de Diego LF, Adánez J. The use of ilmenite as oxygen-carrier in a 500W$_{th}$ Chemical-Looping Coal Combustion unit. International Journal of Greenhouse Gas Control. 2011;5:1630-42.

[31] Linderholm C, Cuadrat A, Lyngfelt A. Chemical-looping combustion of solid fuels in a 10 kW$_{th}$ pilot- Batch tests with five fuels. 2011. p. 385-92.

[32] Markström P, Linderholm C, Lyngfelt A. Operation of a 100kW chemical-looping combustor with Mexican petroleum coke and Cerrejón coal. Applied Energy. 2014;113:1830-5.

[33] Ströhle J, Orth M, Epple B. Design and operation of a 1MW$_{th}$ chemical looping plant. Applied Energy. 2014;113:1490-5.

[34] Thon A, Kramp M, Hartge E-U, Heinrich S, Werther J. Operational experience with a system of coupled fluidized beds for chemical looping combustion of solid fuels using ilmenite as oxygen carrier. Applied Energy. 2014;118:309-17.

[35] Pikkarainen T, Hiltunen I, Teir S. Piloting of bio-CLC for BECCS. 4th International Conference on Chemical Looping. Nanjing, China2016.

[36] Bao J, Li Z, Sun H, Cai N. Continuous Test of Ilmenite-Based Oxygen Carriers for Chemical Looping Combustion in a Dual Fluidized Bed Reactor System. Industrial & Engineering Chemistry Research. 2013;52:14817-27.

[37] Lyngfelt A. 11 - Oxygen carriers for chemical-looping combustion. In: Fennell P, Anthony B, editors. Calcium and Chemical Looping Technology for Power Generation and Carbon Dioxide (CO2) Capture: Woodhead Publishing; 2015. p. 221-54.

[38] Abad A, Mattisson T, Lyngfelt A, Johansson M. The use of iron oxide as oxygen carrier in a chemical-looping reactor. Fuel. 2007;86:1021-35.

[39] Linderholm C, Schmitz M. Chemical-looping combustion of solid fuels in a 100 kW dual circulating fluidized bed system using iron ore as oxygen carrier. Journal of Environmental Chemical Engineering. 2016;4:1029-39.

[40] Song T, Shen T, Shen L, Xiao J, Gu H, Zhang S. Evaluation of hematite oxygen carrier in chemical-looping combustion of coal. Fuel. 2013;104:244-52.

[41] Abad A, Adánez-Rubio I, Gayán P, García-Labiano F, de Diego LF, Adánez J. Demonstration of chemical-looping with oxygen uncoupling (CLOU) process in a 1.5 kWth continuously operating

unit using a Cu-based oxygen-carrier. International Journal of Greenhouse Gas Control. 2012;6:189-200.

[42] Adánez-Rubio I, Abad A, Gayán P, de Diego LF, García-Labiano F, Adánez J. Biomass combustion with CO_2 capture by chemical looping with oxygen uncoupling (CLOU). Fuel Processing Technology. 2014;124:104-14.

[43] Adánez-Rubio I, Pérez-Astray A, Mendiara T, Izquierdo MT, Abad A, Gayán P, et al. Chemical looping combustion of biomass: CLOU experiments with a Cu-Mn mixed oxide. Fuel Processing Technology. 2018;172:179-86.

[44] Rydén M, Jing D, Källén M, Leion H, Lyngfelt A, Mattisson T. CuO-Based Oxygen-Carrier Particles for Chemical-Looping with Oxygen Uncoupling – Experiments in Batch Reactor and in Continuous Operation. Industrial & Engineering Chemistry Research. 2014;53:6255-67.

[45] Adánez-Rubio I, Abad A, Gayán P, Adánez I, de Diego LF, García-Labiano F, et al. Use of Hopcalite-Derived Cu–Mn Mixed Oxide as Oxygen Carrier for Chemical Looping with Oxygen Uncoupling Process. Energy & Fuels. 2016;30:5953-63.

[46] Rydén M, Leion H, Mattisson T, Lyngfelt A. Combined oxides as oxygen-carrier material for chemical-looping with oxygen uncoupling. Applied Energy. 2014;113:1924-32.

[47] Mohammad Pour N, Leion H, Rydén M, Mattisson T. Combined Cu/Mn oxides as an oxygen carrier in chemical looping with oxygen uncoupling (CLOU). Energy and Fuels. 2013;27:6031-9.

[48] Mattisson T, Jing D, Lyngfelt A, Rydén M. Experimental investigation of binary and ternary combined manganese oxides for chemical-looping with oxygen uncoupling (CLOU). Fuel. 2016;164:228-36.

[49] Arjmand M, Frick V, Rydén M, Leion H, Mattisson T, Lyngfelt A. Screening of Combined Mn-Fe-Si Oxygen Carriers for Chemical Looping with Oxygen Uncoupling (CLOU). Energy & Fuels. 2015;29:1868-80.

[50] Shulman A, Cleverstam E, Mattisson T, Lyngfelt A. Manganese/iron, manganese/nickel, and manganese/silicon oxides used in chemical-looping with oxygen uncoupling (CLOU) for combustion of methane. Energy and Fuels. 2009;23:5269-75.

[51] Rydén M, Moldenhauer P, Lindqvist S, Mattisson T, Lyngfelt A. Measuring attrition resistance of oxygen carrier particles for chemical looping combustion with a customized jet cup. Powder Technology. 2014;256:75-86.

[52] Källén M, Rydén M, Dueso C, Mattisson T, Lyngfelt A. $CaMn_{0.9}Mg_{0.1}O_{3-\delta}$ as oxygen carrier in a gas-fired 10 kW_{th} chemical-looping combustion unit. Industrial and Engineering Chemistry Research. 2013;52:6923-32.

[53] Hallberg P, Källén M, Jing D, Snijkers F, van Noyen J, Ryden M, et al. Experimental Investigation of $CaMnO_{3-\delta}$ Based Oxygen Carriers Used in Continuous Chemical-Looping Combustion. International Journal of Chemical Engineering. 2014;2014:9.

[54] Arjmand M, Rydén M, Leion H, Mattisson T, Lyngfelt A. Sulfur Tolerance and Rate of Oxygen Release of Combined Mn–Si Oxygen Carriers in Chemical-Looping with Oxygen Uncoupling (CLOU). Industrial & Engineering Chemistry Research. 2014;53:19488-97.

[55] Hanning M, Frick V, Mattisson T, Rydén M, Lyngfelt A. Performance of Combined Manganese–Silicon Oxygen Carriers and Effects of Including Titanium. Energy & Fuels. 2016;30:1171-82.

[56] Sundqvist S, Arjmand, M., Mattisson, T., Leion, H., Rydén, M., Lyngfelt, A. . Screening of different manganese ores for chemical-looping combustion (CLC) and chemical looping with oxygen uncoupling (CLOU). 11th International Conference on Fluidized Bed Technology, CFB 2014. Beijing; China 2014. p. 893-8.

[57] Linderholm C, Schmitz M, Knutsson P, Lyngfelt A. Chemical-Looping Combustion in a 100-kW Fluidized-Bed System using a Mixture of Ilmenite and Manganese Ore as Oxygen Carrier. Submitted for publication. 2015.

[58] Linderholm C, Lyngfelt A, Cuadrat A, Jerndal E. Chemical-looping combustion of solid fuels – Operation in a 10 kW unit with two fuels, above-bed and in-bed fuel feed and two oxygen carriers, manganese ore and ilmenite. Fuel. 2012;102:808-22.

[59] Sozinho T, Pelletant W, Stainton H, Guillou F, Gauthier T. Main results of the 10 kWth pilot plant operation. 2nd International Conference on Chemical Looping. Darmstadt2012.

[60] Xu L, Edland R, Li Z, Leion H, Zhao D, Cai N. Cu-Modified Manganese Ore as an Oxygen Carrier for Chemical Looping Combustion. Energy & Fuels. 2014;28:7085-92.

[61] Pikkarainen T, Hiltunen I. Chemical Looping Combustion of Solid Biomass - Performance of Ilmenite and Braunite as Oxygen Carrier Materials. 25th European Biomass Conference and Exhibition. Stockholm, Sweden 2017.

[62] Linderholm C, Schmitz M, Knutsson P, Källén M, Lyngfelt A. Use of low-volatile solid fuels in a 100 kW chemical-looping combustor. Energy and Fuels. 2014;28:5942-52.

[63] Rydén M, Moldenhauer P, Lindqvist S, Mattisson T, Lyngfelt A. Measuring attrition resistance of oxygen carrier particles for chemical looping combustion with a customized jet cup. Powder Technology. 2014;256:75-86.

[64] Berguerand N, Lyngfelt A. Design and operation of a 10 kW_{th} chemical-looping combustor for solid fuels - Testing with South African coal. Fuel. 2008;87:2713-26.

[65] Berguerand N, Lyngfelt A. The use of petroleum coke as fuel in a 10 kW$_{th}$ chemical-looping combustor. International Journal of Greenhouse Gas Control. 2008;2:169-79.

[66] Berguerand N, Lyngfelt A. Operation in a 10 kW$_{th}$ chemical-looping combustor for solid fuel—Testing with a Mexican petroleum coke. Energy Procedia. 2009;1:407-14.

[67] Berguerand N, Lyngfelt A. Batch testing of solid fuels with ilmenite in a 10 kW$_{th}$ chemical-looping combustor. Fuel. 2010;89:1749-62.

[68] Markström P, Linderholm C, Lyngfelt A. Chemical-looping combustion of solid fuels – Design and operation of a 100kW unit with bituminous coal. International Journal of Greenhouse Gas Control. 2013;15:150-62.

[69] Linderholm C, Schmitz M, Biermann M, Hanning M, Lyngfelt A. Chemical-looping combustion of solid fuel in a 100kW unit using sintered manganese ore as oxygen carrier. International Journal of Greenhouse Gas Control. 2017;65:170-81.

[70] Linderholm C, Knutsson P, Schmitz M, Markström P, Lyngfelt A. Material balances of carbon, sulfur, nitrogen and ilmenite in a 100 kW CLC reactor system. International Journal of Greenhouse Gas Control. 2014;27:188-202.

[71] Lyngfelt A, Leckner B. A 1000 MWth boiler for chemical-looping combustion of solid fuels – Discussion of design and costs. Applied Energy. 2015;157:475–87.

[72] Linderholm C, Schmitz M, Lyngfelt A. Estimating the solids circulation rate in a 100-kW chemical looping combustor. Chemical Engineering Science. 2017;171:351-9.

[73] de Diego LF, Abad A, Cabello A, Gayán P, García-Labiano F, Adánez J. Reduction and Oxidation Kinetics of a CaMn$_{0.9}$Mg$_{0.1}$O$_{3-\delta}$ Oxygen Carrier for Chemical-Looping Combustion. Industrial & Engineering Chemistry Research. 2013;53:87-103.

[74] Arjmand M, Kooiman RF, Rydén M, Leion H, Mattisson T, Lyngfelt A. Sulfur tolerance of Ca$_x$Mn$_{1-y}$MyO$_{3-\delta}$ (M = Mg, Ti) perovskite-type oxygen carriers in chemical-looping with oxygen uncoupling (CLOU). Energy and Fuels. 2014;28:1312-24.

[75] Alifanti M, Auer R, Kirchnerova J, Thyrion F, Grange P, Delmon B. Activity in methane combustion and sensitivity to sulfur poisoning of La$_{1-x}$Ce$_x$Mn$_{1-y}$Co$_y$O$_3$ perovskite oxides. Applied Catalysis B: Environmental. 2003;41:71-81.

[76] Wang H, Zhu Y, Tan R, Yao W. Study on the poisoning mechanism of sulfur dioxide for perovskite La$_{0.9}$Sr$_{0.1}$CoO$_3$ model catalysts. Catalysis Letters. 2002;82:199-204.

[77] Zhu Y, Tan R, Feng J, Ji S, Cao L. Reaction and poisoning mechanism of SO$_2$ and perovskite LaCoO$_3$ film model catalysts. Applied Catalysis A: General. 2001;209:71-7.

[78] Cabello A, Abad A, Gayán P, de Diego LF, García-Labiano F, Adánez J. Effect of Operating Conditions and H2S Presence on the Performance of CaMg0.1Mn0.9O3–δ Perovskite Material in Chemical Looping Combustion (CLC). Energy & Fuels. 2014;28:1262-74.

[79] Linderholm C, Lyngfelt A, Dueso C. Chemical-looping combustion of solid fuels in a 10 kW reactor system using natural minerals as oxygen carrier. Energy Procedia. 2013;37:598-607.

[80] Markström P, Linderholm C, Lyngfelt A. Analytical model of gas conversion in a 100kW chemical-looping combustor for solid fuels—Comparison with operational results. Chemical Engineering Science. 2013;96:131-41.

[81] Linderholm C, Schmitz M, Knutsson P, Lyngfelt A. Chemical-looping combustion in a 100-kW unit using a mixture of ilmenite and manganese ore as oxygen carrier. Fuel. 2016;166:533-42.

[82] Arjmand M, Leion H, Mattisson T, Lyngfelt A. Investigation of different manganese ores as oxygen carriers in chemical-looping combustion (CLC) for solid fuels. Applied Energy. 2014;113:1883-94.

[83] Lyngfelt A, Kronberger B, Adanez J, Morin JX, Hurst P. The grace project: Development of oxygen carrier particles for chemical-looping combustion. Design and operation of a 10 kW chemical-looping combustor. In: Wilson ESRWKFG, Thambimuthu TMG, editors. Greenhouse Gas Control Technologies 7. Oxford: Elsevier Science Ltd; 2005. p. 115-23.